

Antimicrobial silicones for use as dialysis catheters

Ana Rita Noutel Lorga Gomes

Dissertation
Integrated Masters in Bioengineering
Molecular Biotechnology branch

Supervisor: Dr. Inês C. Gonçalves (i3s)
Co-supervisor: Dr. Artur M. Pinto (i3s/FEUP-LEPABE)

June 2017

© Ana Rita Noutel Lorga Gomes, 2017

This thesis was conducted at:

i3s - Instituto de Investigação e Inovação para a Saúde;
Universidade do Porto



LEPABE/FEUP - Laboratório de Engenharia de Processos,
Ambiente, Biotecnologia e Energia; Universidade do Porto



The work described in this thesis was financially supported by:

Project POCI-01-0145-FEDER-007274 (Institute for Research and Innovation in Health Sciences); Project POCI-01-0145-FEDER-006939 - Laboratory for Process Engineering, Environment, Biotechnology and Energy - LEPABE and NORTE-01-0145-FEDER-000005 - LEPABE-2-ECO-INNOVATION, funded by FEDER funds through COMPETE2020 - Programa Operacional Competitividade e Internacionalização (POCI) and Programa Operacional Regional do Norte (NORTE2020), and by national funds through FCT - Fundação para a Ciência e a Tecnologia; and Project PTDC/CTM-Bio/4033/2014 (NewCat - New biomaterials to prevent infection associated with dialysis catheters), funded by FEDER funds through COMPETE2020 - Programa Operacional Competitividade e Internacionalização (POCI) - and by national funds through FCT - Fundação para a Ciência e a Tecnologia.



Acknowledgements

Gostava de começar por agradecer a todos os meus amigos e colegas que partilharam comigo estes 5 anos, principalmente às “resistentes”, que estiveram sempre ao meu lado nos melhores e nos piores momentos.

Um enorme obrigada à minha orientadora, Dr. Inês Gonçalves, por toda a paciência, apoio e sobretudo disponibilidade. Só espero ter sido tão boa aluna quanto a Inês foi orientadora. Agradeço também ao meu co-orientador, Dr. Artur Pinto, por toda a ajuda e conselhos que me deu.

Muito obrigada ao André Maia, coordenador técnico da Biosciences Screening Unit do i3s, que tornou uma boa parte deste trabalho possível, mostrando sempre disponibilidade para me ajudar a melhorar tudo até ao ínfimo pormenor.

Agradeço a todo o grupo Bioengineered Surfaces que acompanhou o meu trabalho desde o início e me deu sugestões e incentivos para melhorar. Obrigada Cristina, Fabíola, Cláudia, Paula, Catarina, Mariana e Hélia.

À equipa do NewCat deixo um agradecimento especial. Ao Prof. Fernão Magalhães por me ajudar a tomar decisões, à Natacha pela companhia e apoio, à Patrícia por me tirar todas as dúvidas desde o início, à Andreia pelas grandes ajudas que me deu, e finalmente à Inês, a minha companheira dos trabalhos difíceis (e dos não tão difíceis também), um obrigada gigante.

Finalmente, gostava de agradecer ao Ricardo por toda a compreensão e toda a força que me dá, aos meus pais por terem estado incondicionalmente do meu lado não só nestes últimos tempos, mas sempre, e à minha irmã Marta que teve que me aturar todos os dias e que me inspira a dar o meu melhor.

Abstract

Catheter-related infection is a severe issue, being one of the most prevalent types of infection in the hospital setting. Peritoneal dialysis catheters are no exception to this matter. These catheters are usually made of silicone, a polymer which is widely used in the biomedical field. Silicone, however, is hydrophobic and tends to attract bacteria to the surface. Some surface modification strategies are used to avoid bacterial colonization of silicone, but few have been used commercially in the production of catheters.

Graphene-based materials (GBMs) are considered antimicrobial, and can readily act and kill bacteria when immobilized in coatings. However, most of the work that combines GBMs and silicone is directed towards improving its physical characteristics, but not its microbicidal properties.

This work aims to investigate the antibacterial properties of GBM-coated silicone. Ideally these results would culminate in a more antibacterial catheter. Medical grade silicone and graphene nanoplatelets (GNPs) with 5 μm of diameter (GNP-M5) and its respective oxidized form (GNP-M5ox) were used for this purpose. The effect of GNP exposure and oxidation in the antibacterial activity of the coating was investigated. For this purpose, two distinct coating strategies - dip and spray coating - were tested to achieve the exposure of the GNPs at the surface. The GNPs were immobilized either with silicone as a binder, or coated with no binder.

The oxidation of GNP-M5 to GNP-M5ox was successfully performed. The presence of a binder (silicone) in coatings was found to be necessary to immobilize the GNPs on the surface and therefore only these samples were fully characterized. In general, spray coating exposed higher amounts of GNP at the surface and more homogeneously than dip coating, but the latter provided a better adhesion of the GNPs to the surface, despite not inducing changes in surface wettability. Spray coating with GNP-M5 produces a super hydrophobic surface while spraying with GNP-M5ox renders the surface more hydrophilic. Antibacterial testing of dip coating samples suggests that low amounts of GNP do not influence the number of adherent bacteria, but GNPs in the highest concentration tested present more bacteria attachment than control silicone samples. Nevertheless, while SR and SR/GNP-M5 coated samples have a percentage of dead bacteria between 40% and 50%, the samples coated with SR/GNP-M5ox increased bacterial death to 80%. Spray coating samples induced higher bacterial adhesion and less percentage of dead bacteria than dip coating samples. Nevertheless, coating with GNP-M5ox still resulted in higher percentage of dead bacteria, which was around 75% for the best condition.

As such it was possible to conclude that the coatings with oxidized GNP induce more bacterial death, independently of the coating strategy. However, while for dip coating bacterial death is higher for increasing concentrations because more GNP is exposed, for spray coating this is not seen, possibly because GNP are more masked within the coating.

Globally, this work demonstrates the potential use of GNP coatings in silicone for application in peritoneal dialysis catheters with improved antimicrobial properties.

Table of contents

Acknowledgements.....	v
Abstract	vii
Table of contents.....	ix
List of figures.....	xi
List of tables.....	xiii
Abbreviations and Symbols	xiv
CHAPTER I: Motivation and Aim.....	1
1. Motivation and Aim	1
2. Structure of the Dissertation	2
CHAPTER II: Literature Review	3
1. Silicone: preparation, biomedical use and modification	3
1.1. Structure and preparation of silicone	3
1.2. Biomedical application of silicone	6
1.3. Silicone elastomer molding.....	7
1.4. Surface modification of silicone elastomers	9
1.4.1. Physical modification.....	9
1.4.2. Chemical modification: Covalently attached coatings.....	9
1.4.3. Chemical modification: Non-covalent coatings.....	10
2. Modification of silicone elastomers with graphene-based materials	11
2.1. Graphene-based materials (GBMs)	11
2.2. Silicone with GBMs	11
3. Graphene and its derivatives as antimicrobial materials.....	14
3.1. GBM antimicrobial properties.....	14
3.3. Antimicrobial activity of GBMs in coatings	15
3.3.1. Coatings with GBMs.....	15
3.3.2. GBMs coatings on silicone	16
4. Testing antimicrobial properties of biomaterial surfaces	17
4.1. Catheter-related infection	17
4.2. Types of antimicrobial materials	17
4.3. Antimicrobial surface testing	18
4.3.1. Testing on bacteria in suspension	18
4.3.2. Testing on bacteria adhered on surfaces.....	21
CHAPTER III: Materials and Methods	23
1. Materials Production.....	23
1.1. Graphene Nanoplatelets (GNP)	23
1.1.1. Graphene Nanoplatelets	23
1.1.2. Oxidation of Graphene Nanoplatelets.....	23
1.2. Silicone films.....	24
1.3. GNP coatings	24

1.3.1. GNP coating with no binder	24
1.3.2. GNP coating with silicone as a binder	25
2. Materials Characterization	26
2.1. GNP characterization	26
2.1.1. X-ray Photoelectron Spectroscopy (XPS).....	26
2.1.2. Scanning electron microscopy (SEM)	27
2.2. GNP-coated silicone characterization	27
2.2.1. Optical microscopy	27
2.2.2. Rubbing test	27
2.2.3. Washing test.....	27
2.2.4. Scanning electron microscopy (SEM)	27
2.2.5. Water contact angle.....	27
3. Antibacterial Properties Testing	28
3.1. Bacteria and Growth Conditions.....	28
3.2. Antibacterial assessment of materials.....	28
3.2.1. Testing in adherent bacteria	30
3.2.2. Testing in bacteria in suspension	30
4. Statistical analysis	31
4.1. Contact angles	31
4.2. Antibacterial assays.....	31
CHAPTER IV: Results and Discussion	33
1. Graphene nanoplatelets characterization	33
2. GNP-coated silicone	36
2.1. Silicone rubber films.....	36
2.2. GNP coating with no binder	36
2.2.1. Dip coating.....	36
2.2.2. Spray coating	37
3.1. GNP coating with binder and antimicrobial activity	38
3.1.1. Dip coating.....	38
3.2.2. Spray coating.....	46
CHAPTER V: Conclusion and Future Work	55
1. Conclusion.....	55
2. Future Work.....	56
References.....	57
Annexes	65

List of figures

Figure 1. Silicone elastomer processing by (A) extrusion, (B) compression molding, (C) transfer molding, (D) injection molding. ^{32,33}	8
Figure 2. Potential routes of infection in catheters.	17
Figure 3. Different operating mechanisms of antibacterial surfaces.	18
Figure 4. Schematics of the contact method used on: (A) ISO 22196 and (B) ASTM E2180 standards.....	19
Figure 5. Silicone film production.....	24
Figure 6. GNP/solvent dispersion application and material production.	25
Figure 7. SR/GNP dispersion application and material production.	26
Figure 8. Schematics of the antibacterial assay. (A) Surface inoculation and PP film placement for forcing contact with the inoculum; (B) Testing after 24 h incubation.	29
Figure 9. SEM images of the GNP-M5 powder and lyophilized GNP-M5ox. Pictures taken at the magnification of $\times 1000$ and $\times 10000$ (Scale bar = 80 μm and 8 μm , respectively). ...	34
Figure 10. XPS analysis of GNP-M5 and GNP-M5ox. (A) Atomic percentage of carbon and oxygen obtained by analysis of the survey; (B) C1s high-resolution spectrum of GNP-M5; (C) C1s high-resolution spectrum of GNP-M5ox; (D) Contents of chemical groups resulting of C1s spectra fitting.	35
Figure 11. Silicone rubber film. (A) Stereomicroscopy image; (B) SEM image of front view; (C) SEM image of side view. SEM pictures taken at the magnification of $\times 300$. (Scale bar= 200 μm).	36
Figure 12. Stereomicroscopy images of (A) silicone base film and (B) 1 mg/mL GNP-M5 in THF dip coating sample (Scale bar=5 mm).	36
Figure 13. Stereomicroscopy images of (A) silicone base film and (B) 1 mg/mL GNP-M5 in THF spray coating sample (Scale bar=5 mm).	37
Figure 14. Optical microscopy images of (A) silicone base film and (B) 1 mg/mL GNP-M5 in EtOH spray coating sample (Scale bar=1 mm).	37
Figure 15. Stereomicroscopy images of SR/GNP dip coating samples (Scale bar = 5mm)...	38
Figure 16. Optical microscopy images of SR/GNP dip coating samples. Pictures taken at the magnification of $\times 100$ and $\times 400$ (Scale bar=1 mm and 200 μm , respectively).	39
Figure 17. SEM images of SR/GNP dip coating samples. Pictures taken at the magnifications of $\times 300$, $\times 1000$ and $\times 3000$ (Scale bar= 200 μm , 80 μm and 20 μm , respectively).	41

Figure 18. Water contact angle for SR/GNP dip coating samples. Statistical analysis performed by Kruskal Wallis test and statistically significant differences are indicated with * ($p \leq 0.05$).	42
Figure 19. <i>S.epidermidis</i> adherent to SR/GNP dip coating samples after 24 h incubation. (A) Metabolic activity of bacteria in the surface after 3,5 hours incubation with resazurin; (B) Total adhered bacteria per mm^2 ; (C) Percentage of live (green), dying (orange) and dead (red) bacteria; (D) Representative images of the LIVE/DEAD staining (Scale bar=50 μm); (E) Images of bacteria adhered to SR and GNP aggregates (Scale bar=10 μm). Statistical analysis of the metabolic activity assay and total adhered bacteria performed with Kruskal-Wallis test and ordinary One-way ANOVA, respectively. Statistically significant differences are indicated with * ($p \leq 0.05$)......	44
Figure 20. Planktonic <i>S.epidermidis</i> of SR/GNP dip coating samples after 24 h incubation. (A) Metabolic activity of bacteria in suspension after 1 hour incubation with resazurin and (B) colony forming units of the viable bacteria collected in supernatant. Statistical analysis of metabolic activity was performed with Kruskal-Wallis test and CFUs with ordinary One-way ANOVA. Statistically significant differences are indicated with * ($p \leq 0.05$).	45
Figure 21. Stereomicroscopy images of SR/GNP spray coating samples (Scale bar = 5mm).	46
Figure 22. Optical microscopy images of SR/GNP spray coating samples. Pictures taken at the magnification of $\times 100$ and $\times 400$ (Scale bar=100 μm and 20 μm , respectively).	47
Figure 23. SEM images of SR/GNP spray coating samples. Pictures taken at the magnifications of $\times 300$, $\times 1000$ and $\times 3000$ (Scale bar= 200 μm , 80 μm and 20 μm , respectively).	49
Figure 24. Water contact angle for SR/GNP spray coating samples. Statistical analysis performed by Kruskal Wallis test and statistically significant differences are indicated with * ($p \leq 0.05$).	50
Figure 25. <i>S.epidermidis</i> adherent to SR/GNP spray coating samples after 24 h incubation. (A) Metabolic activity of bacteria in the surface after 3,5 hours incubation with resazurin; (B) Total adhered bacteria per mm^2 ; (C) Percentage of live (green), dying (orange) and dead (red) bacteria. (D) Representative images of the LIVE/DEAD staining (Scale bar=50 μm); (E) Images of bacteria adhered to SR and GNP aggregates. (Scale bar=10 μm) Statistical analysis of metabolic activity assay and total adhered bacteria performed with Kruskal-Wallis test and one-way ANOVA, respectively. Statistically significant differences are indicated with * ($p \leq 0.05$)......	52
Figure 26. Planktonic <i>S.epidermidis</i> of SR/GNP spray coating samples after 24 h incubation. (A) Metabolic activity of bacteria in suspension after 1 hour incubation with resazurin and (B) colony forming units of the viable bacteria collected in supernatant. Statistical analysis of metabolic activity was performed with Kruskal-Wallis test and CFUs with ordinary One-way ANOVA. Statistically significant differences are indicated with * ($p \leq 0.05$).	53
Figure 27. Summary of obtained results.....	54

List of tables

Table 1 - Summary of silicone synthesis reactions. ³	3
Table 2 - Composition and polymer linking for each form of silicone.....	5
Table 3 - Biomedical applications of different forms of silicone.	6
Table 4 - Silicone elastomer and GBMs composites: preparation and properties.....	13
Table 5 - Abbreviations used for referring to silicone binder materials.	26
Table 6 - Rubbing test for the dip coatings with no binder. Score of 0 is a clean rubber and 5 is a rubber presenting high GNP detachment.	37
Table 7 - Rubbing test for the spray coatings with no binder. Score of 0 is a clean rubber and 5 is a rubber presenting high GNP detachment.	38
Table 8 - Rubbing test for the SR/GNP dip coating samples. Score of 0 is a clean rubber and 5 is a rubber presenting high GNP detachment.	40
Table 9 - Rubbing test for the SR/GNP spray coating samples. Score of 0 is a clean rubber and 5 is a rubber presenting high GNP detachment.	48

Abbreviations and Symbols

CFUs	Colony forming units
CVD	Carbon vapor deposition
FLG	Few-layer graphene
G	Graphene
GBMs	Graphene-based materials
GNPs	Graphene nanoplatelets
GNP/EtOH	GNP dispersion in ethanol
GNP/THF	GNP dispersion in tetrahydrofuran
GNP-M5	Non-oxidized graphene nanoplatelets
GNP-M5ox	Oxidized graphene nanoplatelets
GO	Graphene oxide
GtO	Graphite oxide
MHM	Modified Hummers method
OD	Optical density
PBS	Phosphate-buffered saline
PDMS	Polydimethylsiloxane
PI	Propidium iodide
PP	Polypropylene
RFUs	Relative fluorescence units
rGO	Reduced graphene oxide
ROS	Reactive oxygen species
RTV	Room temperature vulcanization
SEM	Scanning Electron Microscopy
SR	Silicone film coated with silicone in THF
SRf	Silicone rubber film
SR/GNP	Silicone film coated with GNP and silicone in THF
TCPET	Tissue culture polyethyleneterephthalate
THF	Tetrahydrofuran
TSA	Trypticase soy agar
TSB	Trypticase soy broth
XPS	X-Ray photoelectron spectroscopy

CHAPTER I: Motivation and Aim

1. Motivation and Aim

Silicone is a synthetic polymer and the most used material for peritoneal dialysis catheters in the form of silicone elastomer. This happens because, in general, silicone is an inert material which combines absence of adverse biological reactions with good elastomeric properties. However, silicone catheters have elevated risk of infection as silicone is hydrophobic, making it likely to concentrate bacteria on the surface, facilitating bacterial adherence. Infection related to silicone catheter use in peritoneal dialysis is a significant issue, as it is the most common complication. For this reason, the quest for an infection resistant biomaterial is urgent.

To avoid infection, surface modification of polymers like silicone can be performed to enhance the antimicrobial properties of the original material. From surface oxidation to surface modification with other materials, numerous strategies have been attempted but few have been successful when the modified silicone catheter is tested in the hospital environment.

Graphene has received a great deal of attention due to its excellent mechanical, optical and electrical properties. Recently, graphene and graphene-based materials (GBMs) have been used in other applications like drug delivery and functionalization of other nanomaterials to convey antimicrobial properties. However, GBMs by themselves are generally considered intrinsically antimicrobial. Moreover, their biocompatibility has also been characterized and for low concentrations the toxicity is negligible. For these reasons, GBMs appear as an attractive choice for the development of a more effective antibacterial silicone.

This work focused on exploiting the antimicrobial activity of GBMs, namely graphene nanoplatelets (GNP), as a coating for a potential silicone catheter. GNP with 5 μm in diameter (GNP-M5) and its oxidized form (GNP-M5ox) were used to investigate the influence of the oxidation in the antibacterial properties. Each form of each GNP was produced, characterized and tested for antimicrobial properties. Two different coating strategies, dip and spray coating, were tested in terms of GNP exposure. The influence of the exposure of GNP was also subject of surface antibacterial activity evaluation.

2. Structure of the Dissertation

The present dissertation is organized into four chapters. Chapter I includes the motivation and aim of the dissertation.

Chapter II - Literature Review begins with summarizing aspects related to silicone as a polymer in research and medical field, including its general properties, manufacturing and the modification of the surface of silicone. This is followed by a section dedicated to graphene and graphene-based materials (GBMs) as antimicrobial agents and a review of the literature on silicone modified with GBMs for various purposes. This chapter closes with a section describing techniques to evaluate antimicrobial properties of surfaces.

Chapter III - Materials and Methods covers the materials and the procedures used to perform the work present in this dissertation. The production of oxidized graphene nanoplatelets (GNP) is described in detail. The production of two different approaches for applying GNP dispersion coatings on silicone is also described: using no binder or using silicone as a binder. The dispersions were applied dip coating or spray coating. The presence, distribution and orientation of the GNP on the surface of the samples was assessed. Samples which presented GNP as free, non-bound material on the surface were discarded for further characterization. Samples with good GNP immobilization were used to perform antibacterial testing. Surfaces and supernatants were tested in terms of the viability and metabolic activity of the bacteria. Chapter IV - Results and Discussion compiles the results obtained with the tests mentioned in Chapter III, and the discussion of the latter. The chapter is divided concerning each type of material used as a binder of the GNPs. Regarding the silicone binder surfaces, the antibacterial test results are presented and discussed.

The last chapter, Chapter V - Conclusions summarizes the main conclusions of the work, and reflects on future work.

i) Silica reduction to silicon. As silica (SiO_2) is the natural source of silicon, it needs to be reduced to the elemental silicon (Si) by the carbothermal method.⁴ This process requires great amounts of heat developed by a strong electric current.⁵

ii) Chlorosilane synthesis. Silicon reacts with a chlorinated organic compound at an elevated temperature.⁴

iii) Chlorosilane hydrolysis. Hydrolyzing the chlorosilane leads to the production of a mixture of cyclic and linear oligosiloxanes, and hydrochloric acid.⁴ These oligomers possess a chain that is too short for most applications, and therefore need to be polymerized or condensed into a chain of sufficient length.³

iv) Polymerization and polycondensation. Cyclic organosilanes must be ring-opened and polymerized with help of an acid or basic catalyzer. Linear organosilanes can be combined when catalyzed by acids and bases by condensation of silanol terminals.³

Silicone polymers can form a three-dimensional network by a crosslinking reaction, which leads to the formation of bonds between polymer chains.³ This process is also known as curing or vulcanization. The crosslinking reaction is used to produce silicone gels, elastomers, and resins from silicone polymers.⁶ Three types of crosslinking are usually performed: using radicals, by condensation, or by addition.


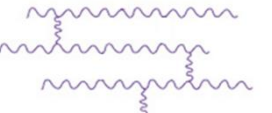
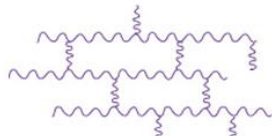
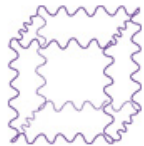
Peroxide radicals are used to crosslink elastomers like silicone and low-density polyethylene which cannot be crosslinked with common curing agents.⁷ The temperature used is high, the crosslinking time is short, and the process results in high consistency glossy silicone rubbers.⁸ However, the volatile residues must be removed post curing to avoid depolymerization.³

There are two types of crosslinking by condensation. In the first type of condensation, the polymer starts crosslinking with contact with moisture, commonly from humidity in the air.⁹ These materials are named one-part RTV (room temperature vulcanization). The second type of condensation reaction relies on the mixing of two components. An organotin salt is used as catalyst and alcohol is released as a by-product.³ Because mixing of two components, a polymer and an silane, is necessary, these are called two-part systems.

Crosslinking by addition is achieved by adding Si-H groups where vinyl groups are present. The addition is catalyzed by Pt or Rh complexes.¹⁰ Platinum cure systems are quickly cured by heat but can be cured at room-temperature. This type of crosslinking also requires the mixture of two parts, and is therefore categorized as a two-part system.³

Depending on the functional group attached to the silicon atom and the degree of crosslinking of the polymer chains, silicones may be categorized into fluids (also known as oils) - the only form of silicone which does not crosslink - gels, elastomers (also known as rubbers) or resins (Table 2).¹¹

Table 2 - Composition and polymer linking for each form of silicone.

Form	Composition	Polymer Linking	Schematic representation
Fluid/Oil	Linear polydimethylsiloxanes (PDMS) Cyclic volatile methylsiloxanes (VMS)	Polymer chains tangle with each other; no crosslinking	
Gel	Silicone fluids; fewer reactive sites and higher molecular weight starting materials	Lightly crosslinked	
Elastomer/Rubber	Linear silicone fluids or gums (thick fluids)	Regular crosslinking	
Resin	Highly branched siloxane polymers	Heavily crosslinked	

Furthermore, in most silicone elastomers, fillers are added to reinforce crosslinking thus enhancing the mechanical strength of the material. The most satisfactory silicone elastomer reinforcement is achieved by using silica fillers.^{8,12} Another common type of filler is carbon black, although it is often used in low-resistivity silicones due to a lower resistivity and thermal stability relatively to silica fillers.¹³

Additionally, carbon nanotubes and graphene-based materials are also being studied as an alternative to commercial fillers.¹⁴ Albeit their similar chemical properties, they possess different morphologies. Multiwalled carbon nanotubes are difficult to disperse in silicone rubber because of their cylindrical shape, which renders the use of 2D-graphene-based materials a more attractive alternative. The production of silicone and GBM composites will be discussed in section 2.

1.2. Biomedical application of silicone

Although hydrophobic, silicone is generally both biocompatible and biodurable, hence the approval of silicone-based gels, elastomers, fluids, and adhesives for medical use by several international agencies.³ This is related to the inertness of the material, and this implies a low interaction with cells and chemicals if inside the body.⁶

Moreover, silicone is also permeable to gases like CO₂ and Oxygen,² which is advantageous for some applications such as contact lenses. In fact, silicones are considered rather unique materials and attractive for medical use, mainly due to the combination of absence of adverse biological reactions and good elastomeric properties.²

Silicones used in medical practice appear in various forms like resin, elastomer, or fluid, which makes various applications possible (Table 3).

Table 3 - Biomedical applications of different forms of silicone.

Application	Description	Silicone form	Ref
Pharmaceutical	Pressure-sensitive adhesives for drug delivery	Resin	15
Ophthalmological	Contact lenses and intraocular lenses	Elastomer	16, 6
Aesthetic	Prosthesis: Finger with matching skin tone	Elastomer	17
	Implants: Breast, testicles, and facial	Elastomer	18, 19, 20
Orthopedic	Interphalangeal and metacarpophalangeal joint replacement	Elastomer	21, 22
Extracorporeal equipment	Membranes for heart bypass machines	Elastomer	23
Gastroenterological	Ring implants for fecal incontinence, esophagus prosthesis	Elastomer	6
Otolaryngologic	Larynx and trachea prosthesis	Elastomer	6
Dermatological	Integra® skin substitutes	Elastomer	24
Cardiovascular	Intravenous (IV) and peripherally inserted central catheters (PICC), cardiac pacemaker leads	Elastomer	1, 25
	Syringe needle lubricant	Fluid	26
Urological	Urinary catheters	Elastomer	27
Nephrological	Peritoneal dialysis catheters	Elastomer	28

The most common silicone used in medical applications is polydimethylsiloxane (PDMS) where the organic groups bound to silicon are two methyl groups.³ Commercial medical-grade PDMS exists in the forms of fluid, gel and elastomer.⁶

One of the main uses of silicone is in catheter production. A catheter is defined as a tubular device designed for insertion into vessels or cavities, to permit the withdrawal or the injection of fluids or other substances.⁸

Silicone has been a main material used for production of various types of central venous access IV catheters (CVC),^{1,29} peripherally inserted central venous catheters (PICC),¹ peritoneal dialysis catheters,³⁰ and urinary catheters.²⁷ Because of its resistance to chemicals and flexibility, silicone has been considered the standard material for long-term access.³⁰ However, for short term use some non-tunneled and non-cuffed silicone acute dialysis catheters are available.²⁸

Silicone as an elastomer appears as the most common form used in biomedical applications. For this reason, this thesis will focus mainly on silicone elastomer use.

1.3. Silicone elastomer molding

As reviewed in section 1.1., silicone elastomers are obtained by crosslinking of low molecular weight, low viscosity silicone polymers.³¹ However, for certain applications, silicone elastomers undergo a molding process before curing, which is used to produce solid elastomers with a pre-determined shape. The elastomers which undergo molding processes are cured by peroxide curing or addition curing, and both processes may be accelerated by heat.³²

There are four main processing methods used with silicone elastomers: extrusion, compression molding, injection molding, and transfer molding (Figure 1). The extrusion process is used with solid silicone elastomer and the molding process is performed either with solid or liquid silicone rubber.³²

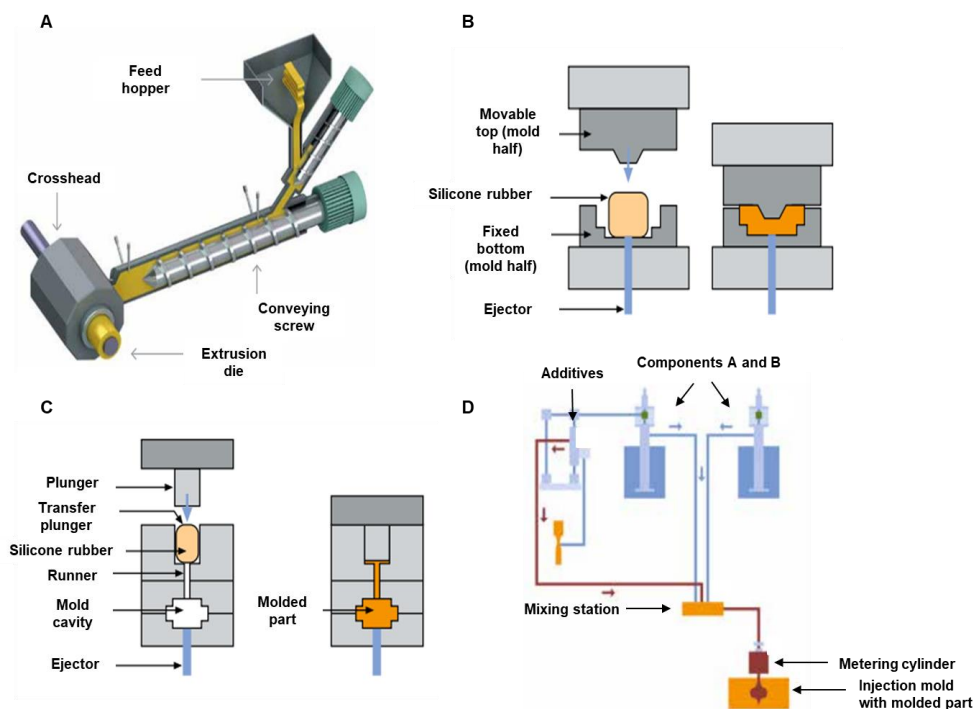


Figure 1. Silicone elastomer processing by (A) extrusion, (B) compression molding, (C) transfer molding, (D) injection molding.^{32,33}

Extrusion of silicone is a process in which the material is squeezed through a die with the help of a conveying screw and is subsequently cured by heat. This process can be used for producing tubes or cables.³²

Compression and transfer molding are both press molding processes. In compression molding, a preform (rough piece of uncured elastomer) is placed on one half of a heated mold.³³ When the mold is closed, the compressed rubber spreads into the entire cavity. In transfer molding, the uncured rubber is placed in a chamber on top of the mold and placed in a press. The pressure forces the rubber to flow through an open end on the pot and spreading into the heated mold. This is useful when avoiding air trapping is crucial.³³

In injection molding, the liquid or solid silicone elastomer components are pumped into a mixer which homogenizes uncured rubber before being forced through a nozzle into a heated, closed mold. This automated process is characterized by its accuracy and the production of high quality parts.³²

1.4. Surface modification of silicone elastomers

1.4.1. Physical modification

The surface of silicone can be modified by physical techniques which generate high energy species or deposit atomic clusters at the surface.³⁴ Some examples are plasma treatments, UV-irradiation, laser treatments, corona treatments, and ion-beam implantation.

Plasma treatments have been used to increase surface wettability, although some hydrophobicity is recovered as cracks in the treated layer of the surface normally occur.³⁵ Different gases such as O₂, N₂, NH₃ and Ar are used, and different excitation frequencies produce different results.³⁶

UV-irradiation in ambient setting leads to the formation of ozone (UV-light in combination with oxygen) and the development of a silicon oxide layer on the surface.³⁷ Silicon oxide films are resistant to oxygen and water, rendering them attractive to use as coatings.³⁸

Laser technology also uses UV frequencies, but with the aim of producing local transformations or patterned surfaces.³⁹

Corona treatments use electrically induced ionized air to bombard the surface of polymers.⁴⁰ It is used to induce oxidation and to improve the overall adhesion properties of silicone.³⁷

Ion-beam implantation on silicone has been considered a breakthrough method in overcoming the usual surface properties of silicone, by improving hydrophilicity and making the surface able to resist biodeposition in long-term use medical devices.⁴¹ In fact the work of Yoshihaki, *et al*⁴² showed that silicone implantation with O₂⁺ ions improved antithrombogenicity.

1.4.2. Chemical modification: Covalently attached coatings

Chemical modification of silicone surface includes modifications by chemical reaction by wet treatment, and covalent bonding of macromolecular chains to the surface, also known as grafting,³⁴ which produces covalently-attached coatings. Out of the two types, grafting is the most commonly used to modify the surface of silicone.²⁵ Grafting is a process based on the activation of the silicone surface by a physical modification technique, such as plasma or ozone treatments. After this step, other molecules can be introduced on the surface with the formation of covalent bonds.

Radiation grafting and photografting have been used to introduce chemically reactive groups onto the surface of hydrophobic, inert polymers like silicone.⁴³ Radiation grafting in particular has been used for various compounds with different applications such as N-vinylpyrrolidone for increasing hemocompatibility,⁴⁴ acrylamide for anti-inflammatory

delivery,⁴⁵ or n-vinylimidazole for antimicrobial properties.⁴⁶ This technique has also been used to produce a patented heparin-grafted silicone surface with anticoagulant properties.⁴⁷

Plasma-induced grafting has been used with PEGMA to avoid bacterial adhesion.⁴⁸ The grafting of an allyl glycidyl ether (AGE) polymer brush by this method has also been applied to attach antimicrobial peptides (AMPs) on the surface of silicone to achieve antimicrobial properties.⁴⁹

Laser induced graft polymerization has been used with pulsed lasers to create concentrated radical areas to effectively graft HEMA on the surface of PDMS to improve the hydrophilicity of the polymer.²⁵

Ozonization, or ozone-induced grafting is a technique which has been used by Xu, et al⁵⁰ for grafting 2-methacryloyloxyethyl phosphorylcholine (MPC) improving hemocompatibility by avoiding platelet adhesion.

1.4.3. Chemical modification: Non-covalent coatings

The production of a thin polymer film on planar surfaces by techniques such as dip coating, spray coating and spin coating has received a great amount of attention recently, owing to the observation of unique properties of thin films compared to bulk materials.⁵¹ However, silicone, due to its relative inertness, is incompatible with most adhesives and coatings, excluding the ones already composed of silicone adhesive and coatings.⁵²

Coating with quaternary ammonium salts (QAS), used to produce antimicrobial surfaces in polymers like silicone,⁵³ can be achieved by spin coating of a solution containing QAS in methanol blended with silicone and the catalyst.⁵⁴ The use of silver alloys in thin film coatings with liquid silicone rubber for conveying antimicrobial properties to catheters has also been described, although no significant decrease of infections was observed.⁵⁵ Dopamine has also been used to produce an antimicrobial coating based on a polydopamine solution (PDA) and silver nanoparticles (AgNP) on the luminal and external surfaces of silicone catheters,⁵⁶ without the need of activating the surface or using silicone in the coating solution. The preparation of the coating in alternate layers of PDA and AgNP ensured a controlled release of the latter.

2. Modification of silicone elastomers with graphene-based materials

2.1. Graphene-based materials (GBMs)

Graphene (G) can be defined as a two-dimensional, single-atom plane of carbon.⁵⁷ Graphene can be synthesized by top-down and bottom-up processes.⁵⁸ Top-down methods include several processes used to exfoliate graphite, namely mechanical, liquid phase, and thermal exfoliation,⁵⁹ and also by the reduction of graphene oxide (GO).⁶⁰ Bottom-up processes, like chemical vapor deposition (CVD), epitaxial growth, and arc discharge use a source of elemental carbon to convert the latter into graphene and graphene-based materials (GBMs).⁵⁹

Other GBMs used in research include graphene oxide (GO), reduced graphene oxide (rGO) and graphene nanoplatelets (GNP). Graphene oxide (GO) consists of a highly-oxidized form of the original graphene. Graphene oxide, and also graphite oxide (GtO), are usually oxidized by Hummers method.^{61,62} GO bears various oxygenated groups, namely hydroxyl and epoxy groups in the basal plane, while at the edges carbonyl and carboxyl groups are present.⁶² Because of this strong oxygenation GO is considered hydrophilic and can be easily dispersed in water and further functionalized.⁶³ Graphene nanoplatelets (GNP), also sometimes named “few-layer graphene” (FLG), are constituted by stacked graphene sheets with a thickness of 2 to 10 layers.⁶⁴ Generally, GNP are 5 to 25 nm thick and can have 0.5 to 25 μm in diameter.⁶⁵

The varied applications of graphene resulting of its mechanical, optical, electrical, and magnetic properties⁶⁶ have led to an increasing development of promising research in the field of Materials Science namely to produce sensors,⁶⁷ or packaging materials.⁶⁸ Moreover, graphene and GBMs have been described as having bactericidal action, a property which made them an attractive choice for designing antimicrobial materials.

2.2. Silicone with GBMs

Most research work performed combining silicone elastomers and GBMs focuses on the production of composite materials intending to achieve a reinforcement of mechanical, thermal, electrical, or adhesive properties of the base silicone material, either with graphene nanoplatelets (GNP), graphene oxide (GO) or graphene. As Table 4 shows, GBMs incorporation in silicone elastomer is commonly achieved by dispersing both silicone and the GBMs independently by sonication in a solvent, such as tetrahydrofuran (THF) or toluene, followed by mixing the GBM dispersion to the base elastomer or the recently cured elastomer. The mixture must be heated to evaporate the solvents before curing.

Other strategies avoid the use of solvents and consist on adding the GBM in liquid rubber or to the base elastomer using a high-speed mixer before curing. The use of silanes for functionalization of GBMs is generally employed to enhance their dispersion in the polymer matrix by changing the physical and chemical properties of the surface of these materials.⁶⁹

Although considerable research has been developed in reinforcing the mechanical properties of silicone with GBMs, little work has been done combining both to achieve a suitable material for implants or medical devices. Graphene nanoplatelets have been combined with silicone in heart valve prosthetics to produce a more mechanically fail-resistant silicone material. The incorporation did not significantly change hemocompatibility or induce cytotoxicity.⁷⁰

Overall, the addition of GBMs to silicone rubber results in the reinforcement of mechanical properties. This may be considered a negative outcome if these materials are employed to develop a novel dialysis catheter, as peritoneal dialysis catheters must be soft and flexible.³⁰ For this reason, a solution based on surface modification of silicone with GBMs might be an alternative approach to this issue. For instance Lin, *et al*⁷¹, deposited a single layer of graphene by transfer coating on different substrates, including PDMS with two degrees of increasing stiffness. All substrates coated showed good cytocompatibility, although the stiffer the substrate, the strongest was the adhesion and the proliferation of fibroblasts. Min, *et al*⁷² also used rGO in an ethanol dispersion for spray coating in PDMS electrodes as a substitute for carbon paste, which yielded much more flexible electrodes. This work suggests GBM coatings do not alter the physical properties of the base PDMS material.

Table 4 - Silicone elastomer and GBMs composites: preparation and properties.

GBM	Silicone	Mixing and curing conditions	Enhanced properties	Ref
APTES, VTMS or Triton X functionalized GNP	MVSR	Disperse both components in THF with sonication (2h) Mix both and sonicate (2h) Evaporate THF at 65°C and cure at 165°C	Mechanical Thermal	73
Graphene nanoribbons (GNR)	MVSR	Disperse both components in THF with sonication (GNR for 6h and silicone for 2h) Mix both and sonicate (2h) Remove THF at 60°C and cure at 170°C	Mechanical Thermal	74
GNP	Liquid rubber	Disperse with Dispermat (500 rpm, 1h) Add catalyst Cure at room temperature for 20h	Thermal	75
GNP	MVSR and Hydroxyl silicon fluid	Use internal mixer to mix all components (20 min, 90 rpm, 105°C) Further mixing Speed Mixer (3000 rpm, 5min) Add curing agent and mix in internal mixer Cure at 120°C	Electrical Mechanical Thermal	76
GNP	PDMS	Disperse GNP in acetone for 1 h and add to base Add activator and cure	Mechanical	70
TEVS - GO	PMVS PMHS	Sonicate GO in toluene (2h) Mix with PMVS Cure at 80°C	Mechanical Thermal	77
GO	PDMS	Disperse both components in toluene Mix and sonicate (1h) and add TEOS Add catalyzer and cure at room temperature for 7 days	Mechanical Thermal	78
Reduced GO (rGO)	PDMS	rGO added to part A (base elastomer) by Speed Mixer then add part B Cure at 180°C	Electrical Mechanical	79
GO and rGO	PMVS	1 phr RGO and GO ultrasonicated in ethanol; milled on two roll mill Add to 100 phr silicone gum and mill Remove ethanol at 60°C for 48h Mill and add curing agent Cure at 180°C	Thermal	80
Functionalized graphene (fG)	PDMS	Add PDMS gum and catalysers and stir (2h) Add fG and stir (3h) Pour into Teflon mold and cure at 110°C	Mechanical Thermal	81
γ -APTES functionalized graphene oxide (fGO)	dihydroxyPDMS	Disperse fGO in acetone/water (9/1) Disperse PDMS in cyclohexane Ultrasonicate for 6 h Catalyse and cure at RT Reduce with hydrazine hydrate to fG/RTV and heat at 100°C	Mechanical Thermal	82
Functionalized graphene sheets (FGS) (thermally exfoliated GO)	PDMS	Manually mix FGS into uncrosslinked PDMS (15 min) Add curing agent and mix (5 min) Cure at 150°C or 160°C	Mechanical	83
GO and graphene	PDMS	GO and graphene mixed and pumped into a container Cure at 80°C for 2h	Adhesive	84

APTES: (3-Aminopropyl)triethoxysilane; MVSR: Methyl-vinyl silicone rubber; PDMS: Polydimethylsiloxane; PMVS: Polymethylvinylsiloxane; PMHS: Polymethylhydrosiloxane. TEVS: Triethoxyvinylsilane; VTMS: Vinyltrimethoxysilane.

3. Graphene and its derivatives as antimicrobial materials

3.1. GBM antimicrobial properties

Intrinsic physicochemical properties of the GBMs such as state of dispersion, size, shape, and layer number are possible factors influencing their antimicrobial activity. Furthermore, the mechanisms by which graphene based materials exert their antibacterial action is also controversial.

It is not surprising that the activity of GBMs highly depends on disaggregation of the materials.⁸⁵ As they possess high surface energies, their separation is vital to maintain shape and high surface area. Concerning size, the results are conflicting. Different results are reported especially when comparing GBMs in solution and in coatings. When in solution, larger graphene and GO sheets appear to entrap bacteria, causing the decrease in viability.⁸⁶ This is the so-called membrane-wrapping mechanism. However, it is likely that this process is reversible, as live bacteria were found inside aggregated sheets of graphene after sonication.⁸⁷ But when present in coatings, small-sized sheets are more effective and pierce the cell membrane on contact⁸⁶. This blade-like action of sharp edges present on GBMs is one of the most agreed mechanisms which cause bacterial death. This happens due to the leakage of intracellular materials and cell death.⁸⁵ However, when present in thin films, the edges may merge together and this effect is limited.⁸⁸ Regarding the number of layers, typically thinner, few-layered GBMs are easier to disperse and readily act as a membrane-piercing structure.⁸⁵

The production of ROS and death by oxidative stress is also viewed as a favorable mechanism although no consensus has been achieved among the scientific community. The presence of O₂ in oxidized GBMs and the introduction of these groups in the bacteria generate ROS and subsequent lipid peroxidation, mitochondrial dysfunction and protein inactivation.⁸⁵ Additionally, bacteria are capable of reducing the oxygen species present in the materials and passively contributing to their own death; this is called the self-killing effect.⁸⁵ However, other groups support the theory of oxidative stress induced by electron transfer rather than by ROS production.⁸⁸

Other conditions unrelated to the materials, such as the presence of analytes, ions and different pH in the solution, and the microbial strain used is also believed to influence the outcome of the activity of GBMs on bacteria.⁸⁵ The thickness of the bacterial wall (Gram-positive or Gram-negative) and the cell shape (coccus or bacillus) may affect the sensibility of one strain of bacteria more than another. Typically, Gram-positive bacteria react differently to the same material when compared to Gram-negative bacteria. The use

of GBMs in nanocomposites as a way of improving their antibacterial action has been extensively explored using a range of materials, including metals, metal oxides and polymers, as described in various reviews.^{87,89-91} These nanocomposites have been tested in solution, films, composite matrices and coatings.

3.3. Antimicrobial activity of GBMs in coatings

Both GBM and GBM nanocomposites have been used in coatings for various materials for electrical, sensing or protective purposes, using diverse coating methods.⁶⁰ The antimicrobial activity attributed to GBMs has also been explored in coatings.

As reviewed in the previous sections, small, few-layer GBMs tend to work best in coatings. Ideally, their sharp edges should be exposed. However, other factors are important when considering developing antibacterial coatings. One of the factors is hydrophobicity. Bacteria tend to attach to hydrophobic surfaces which implies more adhesion to a surface with graphene and less adhesion to amphiphilic GO-coated surfaces.⁸⁶ Another factor is the roughness of the coated surface, as an increasing in roughness attracts more bacteria. This can be positive if the surface is bactericidal but undesirable if the surface is designed to avoid bacterial adhesion.⁸⁶

Ultimately, with all varying features and mechanisms, it is crucial to pick the best GBM for a specific application. The following section reviews work performed on GBMs used in coatings.

3.3.1. Coatings with GBMs

GBMs can be coated on surfaces by themselves deposited as a thin film. CVD-deposited graphene (G) on conductive Cu and Ge substrates and isolating SiO₂ substrates produced different results on antibacterial properties.⁸⁸ While G-Cu and G-Ge induced membrane damage and hindered *E. coli* and *S. aureus* proliferation, G-SiO₂ did not. Because the latter is isolating, the theory of charge transfer was proposed as the main disruptor of the bacterial membrane. However, other work performed by Parra, *et al*⁹² discredited the theory of charge transfer, as a single-layer graphene conductive layer coated over a Cu substrate suppressed charge interaction with bacteria, contrarily to what was detected on the uncoated Cu substrate and similarly to what was seen on an isolating hexagonal-boron nitride coating. Titanium-niobium (Ti-Nb) alloy coated with graphene oxide (GO) by dip coating also produced antibacterial action against *E. coli*.⁹³ The authors discarded the charge transfer theory and proposed bacterial reduction of GO as the main killing mechanism. Still concerning GO, Perreault, *et al*⁹⁴ proposed that when present in coatings, GO loses its ability to pierce membranes and alternatively interaction with basal

planes is enhanced. The importance of oxidative stress was also denoted, although the differences in coating and in suspension still remain unclarified.

Various work has been performed using polymers to embed GBMs in membranes and coatings. Generally, as the GBM content increases, the antibacterial activity is enhanced.⁸⁶ Santos, *et al* developed a coating for metal surfaces based on GBMs and poly(N-vinylcarbazole) (PVK).^{95,96} The authors propose a synergistic antibacterial effect of PVK possibly derived from the better state of dispersion of graphene, and morphological and electronic modifications due to interaction with the polymer. PVK-GO induced 90% more bacterial death and PVK-G inhibited 80% of biofilm formation. GO-sheets embedded in an alkyd resin also inhibited *E. coli*, *P. aeruginosa*, and *S. aureus* viability for at least 69% after 24 h and 85% after 48 h of contact.⁹⁷

Because of the successful immobilization of GBMs in coatings, nanocomposites with GBMs also began to be tested with the same purpose. GO and gelatin-functionalized GO deposited on nitinol inhibited *E. coli* growth, with the membrane integrity being successfully documented in SEM images.⁹⁸ The combination of GBMs with materials which are already antibacterial is a common way of achieving the enhancement of these properties. Graphene conjugated with TiO₂ nanoparticles deposited on cotton fabric improved the antibacterial activity of the nanoparticles, possibly by increasing contact with the bacteria due to its high surface area.⁹⁹ GO combined with antibacterial silver nanoparticles (AgNPs) lead to an inactivation of *E.coli* and damaging of its cellular membrane after contact for 2 h.¹⁰⁰ Silver/hydroxyapatite/graphene composite coatings electrodeposited on titanium reduced bacterial growth of *S. aureus* and *E. coli* after only 3 h of exposure.¹⁰¹

3.3.2. GBMs coatings on silicone

To this date, very few research has been published related to work on the combination of silicone and graphene towards an antimicrobial material. Nonetheless, one article published by Correa, *et al*¹⁰² reports the successful production of an antimicrobial PDMS containing two fillers: titanium dioxide and/or graphene oxide. GO and TiO₂ were added to the silicone by dripping a solution of absolute ethanol on the top of the material, producing a coating, or by homogenizing both silicone and solution by stirring. Although PDMS/GO showed one of the two best results for antimicrobial and antifungal activity, the authors did not clarify which method of GO exposure produced the best outcome.

4. Testing antimicrobial properties of biomaterial surfaces

4.1. Catheter-related infection

Infection related to medical devices is a relevant issue, accounting for 25,6% of healthcare associated infections in 2011.¹⁰³ Dialysis catheter-related infection in particular is related to as much as 26% of these cases.¹⁰⁴ The main routes of infection for catheters are depicted in Figure 2.

Because of its inherent hydrophobicity, PDMS-based devices (including catheters) have the disadvantage of having low wettability and biofouling due to non-specific analyte adsorption and bacterial adhesion.¹⁰⁵

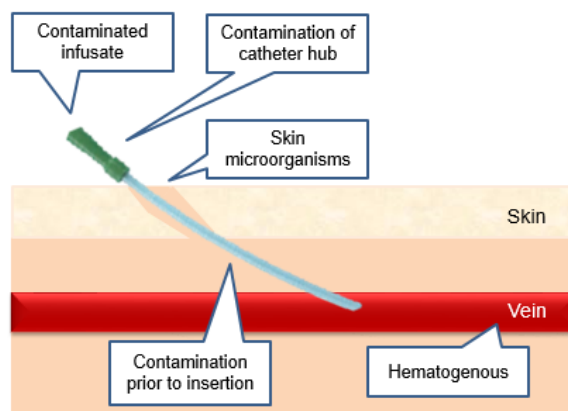


Figure 2. Potential routes of infection in catheters.

The formation of a biofilm on a device or an implant is also a relevant event which culminates in the development of infection.¹⁰⁶ A biofilm can be defined as an aggregate of a single or multiple microbial species attached to a surface.¹⁰⁷ The formation of a biofilm in intravenous or urinary catheters is no exception.^{55,108}

Several approaches have been developed to avoid bacterial attachment and proliferation on biomaterial surfaces in order to lower the risk of infection.¹⁰⁹ These strategies are briefly described in the following section.

4.2. Types of antimicrobial materials

Antibacterial surfaces can be divided into categories depending on their operating mechanism: bactericidal surfaces for killing bacteria, bacteria-resistant surfaces for avoiding attachment, and bacteria-release surfaces for reducing adhesion and enabling the

release of the bacteria already attached by an external force.¹¹⁰ The different categories are depicted in Figure 3.



Figure 3. Different operating mechanisms of antibacterial surfaces.

However, depending on the application, the antibacterial surface requirements are different for distinct types of biomaterials.¹¹¹ A few antimicrobial strategies based on surface modification of silicone - either by rendering the surface more hydrophilic or by means of a coating - have been described in a previous section.

Nonetheless, it is vital to make use of techniques which evaluate the antimicrobial properties of all developed materials to validate their further use in clinical trials. The following section will review the strategies currently used to test these properties in biomaterial surfaces.

4.3. Antimicrobial surface testing

4.3.1. Testing on bacteria in suspension

4.3.1.1. Standardized testing

ISO 22196 is a standard procedure for the measurement of antimicrobial activity on the surface of plastics and non-porous materials.¹¹² The procedure starts with the preparation of pre-culture using predefined bacterial strains and preparation of the specimens. The surfaces to test, both treated and untreated and with no more than 10 mm of thickness, are cut into 50 mm x 50 mm specimens and subsequently cleaned. Testing should be performed on no less than three specimens for each material tested. The test material surfaces are prepared on Petri dishes and later inoculated with 0,4 mL of a bacterial inoculum with the concentration of 6×10^5 cells/mL. A piece of film that measures 40 mm x 40 mm is used on top of the specimen to force contact between bacteria and the surface and avoid evaporation (Figure 4A). The surface is subsequently incubated at $(35 \pm 1)^\circ\text{C}$ for 24 hours. Bacteria are recovered from the surface immediately after inoculation and after incubation. In the first case, the recovery rate of the bacteria is investigated. The process is equal for both recovery processes. Firstly, the volume of 10 mL of a neutralizer broth is used to wash the surface by collecting and release this volume (pipetting up-and-down) at least four times. The supernatant is then collected and 10-fold

dilutions are prepared to inoculate agar plates. The evaluation of bacterial viability is performed as described in 4.3.1.2.

The ASTM E2180 test is used as a standard method for the determination of antimicrobial activity in polymeric or hydrophobic materials.¹¹³ The surfaces, both treated and untreated, are inoculated with 1 mL of the test organism mixed with a semi-solid agar (1 mL of $1-5 \times 10^8$ cells/mL suspension in 100 mL of agar) to achieve surface interaction (Figure 4B). The surfaces must be 30 mm x 30 mm and pre-wetted with a cotton swab dipped in 0,85% saline. The samples are then incubated for 24h at the optimal temperature for the test organism. The procedure for recovery of bacteria from the surface is similar to the ISO 22196 test - one happens immediately and the following at the end of the incubation period. Following the end of incubation, the samples are removed to a container with neutralizing broth and subsequently sonicated and mechanically vortexed to allow complete release of the agar slurry. Subsequent serial dilutions are performed and plated. The evaluation of bacterial viability is performed as described in 3.3.1.2.

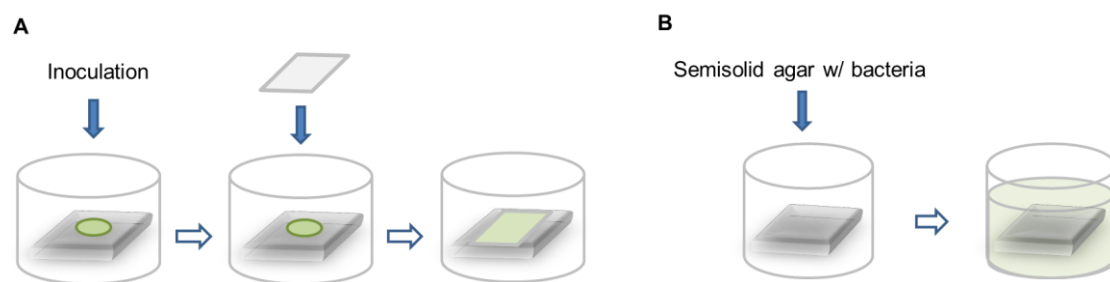


Figure 4. Schematics of the contact method used on: (A) ISO 22196 and (B) ASTM E2180 standards.

4.3.1.2. Colony forming units (CFU) counts

Colony Forming Units (CFU) counting on plates is the gold standard used for bacteria quantification.¹¹⁴ The determination of absolute bacterial number is obtained from plating a bacterial suspension with subsequent incubation. The bacterial colonies resulting from the incubation of the plates are then counted. The results are reported as CFU/mL of suspension.

4.3.1.3. Direct contact test

Correa, *et al*¹⁰² evaluated antimicrobial activity by a direct contact test. Disks of the material are incubated with bacteria on 96-well plates for 24h at 37°C. Once this step finishes, culture medium is added to each well and the plate is shaken. The suspension is

recovered, serial dilutions are performed and plated. CFU are then counted after 24 h of incubation at 37°C.

4.3.1.4. Microcalorimetry

Using this method the production of heat by bacteria due to the presence of metabolic activity is being monitored in a continuous manner by a microcalorimeter.¹¹⁵

In the work of Rio *et al*,¹¹⁶ the correlation between the concentration of MRSA and the peak heat was obtained by measuring the heat flow curves and finding the time-to-peak heat in suspension for materials incubated with serial dilutions (10^7 to 10^2 CFU) by inserting the samples into an ampoule containing broth. The data acquired is reproducible and consistent with growth rate and lag phase data obtained by usually performed OD readings and CFU counts.¹¹⁷

After incubating MRSA on a concentration of 10^6 CFU on Cu-unspattered and antibacterial Cu-spattered polyester, the peak heat was lower than expected and the time-to-peak heat was delayed for the antibacterial material, showing a reduction of at least 4 times- \log_{10} reduction from the initial bacterial concentration in one hour.

4.3.1.5. Metabolic activity assays

Some metabolic activity assays used for eukaryotic cells like the MTT, XTT, or the Resazurin assay can be used or adapted to determine bacterial viability.

The MTT assay relies on the reduction of a tetrazolium salt, MTT (3-(4,5-dimethylthiazol-2-yl)-2,5-diphenyltetrazolium bromide) by growing cells to produce a formazan product, which is blue. The absorbance of the solution containing the blue product is then measured at the wavelengths between 500 and 600 nm.¹¹⁸ However, with bacteria the results may vary even when made routinely. The group of Wang, *et al*¹¹⁹ found that the formazan crystals quickly produced by bacterial reduction aggregate on the bottom of the wells and may entrap cells in the process and compromise the reduction of the remaining reagent. Another tetrazolium salt, the 2,3-bis(2-methoxy-4-nitro-5-sulfophenyl)-5-[(phenylamino) carbonyl]-2H-tetrazolium hydroxide (XTT) is also used for bacterial viability assays, equally relying on the production of the formazan product and absorbance measuring.¹²⁰ XTT does not form formazan crystals, as its product of reduction is soluble.¹²¹

Resazurin is a blue dye that becomes pink and fluorescent when reduced to resorufin by viable cells.¹²² A resazurin test has been used for decades to trace bacterial and yeast contamination of milk.¹²³ For this reason, resazurin has also been used in research, particularly in the investigation of the efficacy of antimicrobial agents.^{122,124}

4.3.2. Testing on bacteria adhered on surfaces

4.3.2.1. Standardized testing

In ISO 22196, when the recovery of bacteria is not sufficient, bacteria must be detached from the surface.¹¹² Mechanical agitation performed by stomaching, vortexing or sonicating show a recovery rate similar to the one described in 4.3.1.1.

4.3.2.2. Direct transfer to agar plates

With this method, the pre-inoculated surfaces are placed in agar plates with the side with the adhered bacteria facing the agar. Some pressure is applied to the surface for 1 minute. The agar plates are then incubated for 16h at 37 °C and the colonies transferred are counted.¹¹⁶

4.3.2.3. Fluorescence-based assays

Fluorescent dyes which bind to nucleic acids can be used to count bacteria adhered to the surface of materials. The 4'-diamidino-2-phenylindole (DAPI) dye has been used for this purpose as a way of screening antifouling agents.¹²⁵ DAPI produces a bright blue fluorescence when bound to DNA, having a great affinity for the A-T rich regions of the latter.¹²⁶ The Hoechst stain has also been used to stain and evaluate the attachment of planktonic bacteria.¹²⁷ It also stains the cells blue and possesses high affinity for the A-T rich regions of DNA, but it is less toxic and more permeable than DAPI.¹²⁶ Both dyes are compatible with living cells, although DAPI can also be used with fixed cells.^{126,128}

Fluorescence-based viability assays are based on stains designed for labelling living and dead cells. One example is the BacLight® LIVE/DEAD kit which uses two fluorophores: SYTO9 which attaches to membranes of living cells and stains the cells with green, and propidium iodide (PI) which has affinity for nucleic acids of dead cells, with compromised membranes, and stains them with red fluorescence.¹²⁹ This stain can be applied on any type of sample with no incubation needed. Hoechst can also be used with PI to assess cell viability.¹²⁶

The use of PNA FISH fluorescent probes directed towards rRNA has also been tested for evaluation and discrimination of the different populations of microorganisms in a biofilm grown on various materials including silicone rubber.¹³⁰

4.3.2.4. Cell morphology evaluation

The effect of antimicrobial agents may produce changes in bacterial morphology indicative of cell death such as bulging or filamentation, which can be observed on surfaces by optical microscopy, scanning electron microscopy (SEM) or transmission electron microscopy (TEM).¹³¹

4.3.2.5. Biofilm formation assays

Several methods have been used to assess biofilm formation on the surface of biomaterials. These methods include SEM and viable cell counts,¹³² and both have also been described here as methods to evaluate bacterial adhesion.

The crystal violet assay uses a crystal violet solution to stain and detect biofilm formation. This assay assesses the total amount of biofilm formed including cell polymeric substances and dead cells.¹³²

The previously described MTT assay has also been used to assess biofilm formation.¹³³

CHAPTER III: Materials and Methods

1. Materials Production

1.1. Graphene Nanoplatelets (GNP)

1.1.1. Graphene Nanoplatelets

Graphene nanoplatelets (xGnP[®] Graphene Nanoplatelets Grade M) were purchased from XG Sciences (Lansing, USA). GNP grade M (GNP-M) have a surface area of around 120-150 m²/g and an average thickness of 2 to 10 layers of graphene. GNP-M with 5 μm of diameter (GNP-M5) was used in this work.

1.1.2. Oxidation of Graphene Nanoplatelets

The widely applied modified Hummer's method¹³⁴ (MHM) was used to oxidize GNP-M5 to GNP-M5ox. The GNP to KMnO₄ ratio used was of 1:6.

4 g of GNP-M5 were added to a mixture of 160 mL of 95-97% H₂SO₄ (VWR, Germany) and 40 mL of H₂PO₄, as proposed by Marcano¹³⁵ for an improved oxidation, while stirring at room temperature. The solution was cooled down using an ice bath to the temperature of 0°C before adding 24 g of KMnO₄, as this reaction is highly exothermic. The resultant mixture was kept under stirring for 2 hours at no more than 35°C. 600 mL of distilled water was then slowly added to the cooled mixture under stirring. Temperatures above 35°C should be avoided. This step was followed by the addition of 35% H₂O₂ until no gas (oxygen) was released. After overnight resting, the mixture was decanted to separate the acidic solution from the oxidized GNP (GNP-M5ox). Other decantations were performed after the GNP-M5ox fully deposited on the bottom of the flask over the next day. The obtained GNP-M5ox was washed by sequentially resuspending in distilled water and centrifuging (4000 rpm, 20 minutes) until the decanted washing water had a pH close to the one of the distilled water (usually around 5). Approximately 6 to 8 washes were required to achieve this pH. The washed GNP-M5ox was then kept in distilled water in a plastic flask.

The concentration in water of the final oxidized GNP was determined by drying a known volume of GNP suspension in a vacuum oven (MMM Group, Germany) at 70 °C overnight. The container of said volume was weighed previous and following the evaporation of the water in the solution to evaluate the mass of GNP-M5ox present.

1.2. Silicone films

MDX4-4210 medical grade silicone elastomer (Dow Corning, USA) with an addition cure system based on platinum curing was used to produce silicone films (Figure 5). Platinum assures the biocompatibility of the polymer. Silica filler was part of the composition of this silicone. 10 parts of base elastomer (9 g) and 1 part of curing agent (1 g) were weighed into separate containers and then thoroughly mixed, according to manufacturer instructions. The mixture was poured into the top of the lid of a 24-well culture plate (Corning, USA) and spread with a glass rod to fully cover the lid. Trapped air bubbles were removed from the film on a vacuum oven and the latter was subsequently cured at 65°C for 2 hours. The film was then cut into 1.5 cm x 1.5 cm square samples.

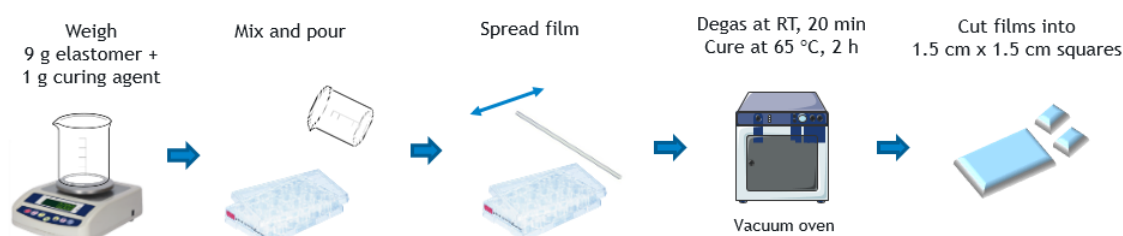


Figure 5. Silicone film production.

1.3. GNP coatings

1.3.1. GNP coating with no binder

Ethanol (EtOH) and tetrahydrofuran (THF) were picked based on the literature to test the dispersion of GNPs. EtOH was used to perform spray coating with rGO,⁷² while THF is a commonly used solvent to disperse GBMs in silicone for composite preparation.

To produce the dispersions for coating, GNP in the reduced form (GNP-M5) was weighed to a beaker to be resuspended in THF or EtOH (JMGS, Portugal). The GNP/THF or GNP/EtOH solution was ultrasonicated 3x 1.5 min on an ice bath to prevent solvent evaporation due to the produced heat. The obtained dispersion in THF was used for dip and spray coating, while the EtOH dispersion was only tested for spray coating (Figure 6). The concentration of 1 mg/mL of GNP-M5 was chosen as the initial testing concentration for all dispersions.

For dip coating, the square silicone film was immersed for 15 s and subsequently dried at 65 °C for 2 h in a vacuum oven. For spray coating, a volume of 6 mL of dispersion was sprayed in a back and forth horizontal motion with an aerograph with a nozzle of 0.2 mm, using air pressure at 1,7 bar. The sample was fixed vertically on the wall.

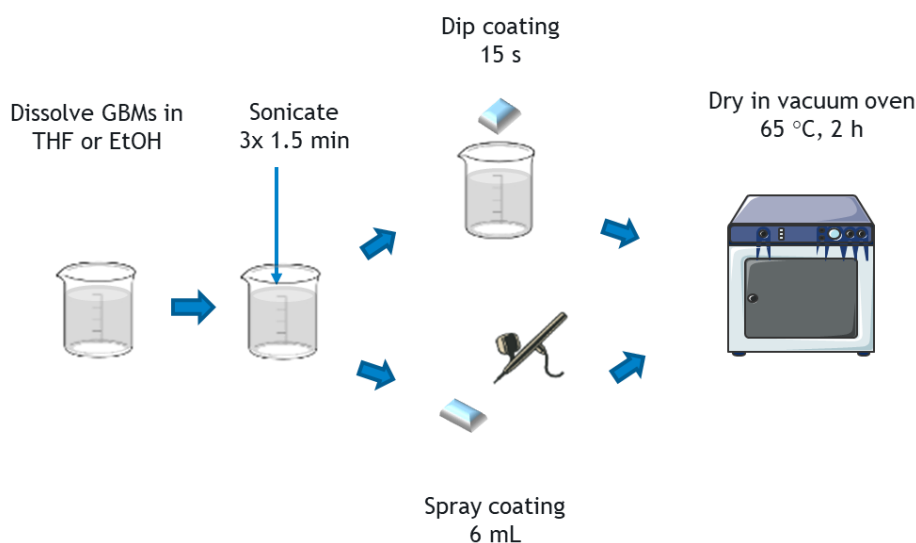


Figure 6. GNP/solvent dispersion application and material production.

1.3.2. GNP coating with silicone as a binder

GNP-M5 was weighed to a beaker, while the GNP-M5ox form needed to be centrifuged from the aqueous solution and washed one time with THF to obtain a certain amount of oxidized material. The GNPs were then dispersed in THF. The elastomer base and curing agent were weighed with the help of a positive displacement pipette (Gilson, USA) onto 2 separate flasks. The proportion recommended by the manufacturer was maintained (10:1). A freshly sonicated GNP/THF dispersion was firstly added to the elastomer base and stirred with a magnet for 10 minutes. The former solution was then added to the flask containing the curing agent and stirred for 10 minutes.

The concentrations of GNPs tested are: 0.5, 1 and 2 mg/mL. The silicone and GNP weight proportion was always kept at 1:1. The resulting silicone/GNP (SR/GNP) dispersion was used for dip and spray coating as described previously (Figure 7). Table 5 summarizes abbreviations which will be frequently used to refer to silicone binder coatings.

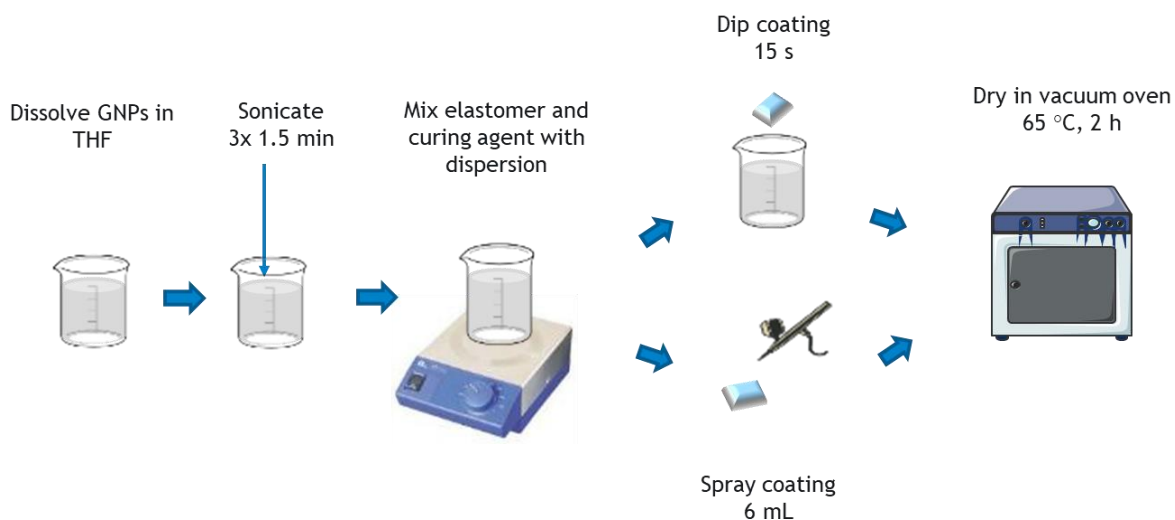


Figure 7. SR/GNP dispersion application and material production.

Table 5 - Abbreviations used for referring to silicone binder materials.

<i>Abbreviature</i>	<i>Meaning</i>
SRf	Silicone rubber base film
SR	Silicone coated with silicone in THF
SR/GNP	Silicone coated with silicone and GNP in THF

2. Materials Characterization

2.1. GNP characterization

2.1.1. X-ray Photoelectron Spectroscopy (XPS)

GNP-M5 and GNP-M5ox were analyzed by X-ray photoelectron spectroscopy (XPS) in order to investigate the elemental composition and state of oxidation. The analysis was performed at CEMUP (Centro de Materiais da Universidade do Porto) using Kratos Axis Ultra HSA equipment. The X-ray produced by an Al monochromator operated with 15 kV power. The survey spectrum was obtained at 80 eV and the elemental spectra (C, O, and S) at 40 eV. The spectra were post processed by deconvolution using CasaXPS software. The peaks were fitted using a Gaussian-Lorentzian shape and a Shirley background.

2.1.2. Scanning electron microscopy (SEM)

The morphology of GNP-M5 powder and GNP-M5ox film was characterized by scanning electron microscopy (SEM) using a Phenom XL desktop SEM at ARCP (Associação e Rede de Competência em Polímeros). The samples were mounted in carbon tape and sputtered with an Au/Pd thin film, usually applied for non-conductive samples.

2.2. GNP-coated silicone characterization

2.2.1. Optical microscopy

Samples were photographed using an Olympus (Olympus, Japan) stereomicroscope at i3s. Samples were also observed under bright field using an Olympus IX51 Inverted Fluorescence Microscope (Olympus, Japan) to evaluate the overall distribution of the GBMs in the sample. Pictures of the samples were taken at $\times 100$ and $\times 400$ magnifications.

2.2.2. Rubbing test

A common white rubber was gently passed through the samples once to investigate if the GNPs in the coating were well adhered to the surface. The color on the rubber resulting from this action was classified on a scale of 0-5, being 0 a white (clean) rubber and 5 a rubber presenting high GNP detachment.

2.2.3. Washing test

Samples were inserted in 50 mL Falcon tubes filled with 30 mL of dH₂O and subjected to 5 s vortexing at maximum speed, for a total of three times. The water from the washing was visually inspected for GNP aggregates and the surface was evaluated in terms of damaging.

2.2.4. Scanning electron microscopy (SEM)

The topography and distribution of GBMs in the sample were analyzed by SEM using a Phenom XL desktop SEM at ARCP (Associação e Rede de Competência em Polímeros). The samples were mounted in carbon tape and sputtered with an Au/Pd thin film, usually applied for non-conductive samples.

2.2.5. Water contact angle

The hydrophobicity of the samples was studied by optical contact angle using water as the test liquid. A volume of 8 μ L was dispensed by a syringe. The sample used for

testing was kept in a chamber with controlled temperature (approximately 25 °C) to avoid the evaporation of the test drop. The detection of the contact angle was performed by the SCA20 software. The measurements were performed in 3 replicas for each sample.

3. Antibacterial Properties Testing

3.1. Bacteria and Growth Conditions

Staphylococcus epidermidis (ATCC 35984) were grown in solid Trypticase Soy Agar (TSA, Merck) plates overnight at 37 °C in a drying oven (Binder, Germany). The colonized plate was then kept at 4 °C up to one week maximum until use.

To produce a liquid inoculum, one or two colonies were collected and resuspended into 5 mL of Trypticase Soy Broth (TSB, Merck) and cultured at 37 °C overnight in an orbital shaker at the speed of 150 rpm.

3.2. Antibacterial assessment of materials

To assess the antibacterial activity of the materials, an adapted protocol for the standard “ISO 22196 - Measurement of antibacterial activity on plastics and other non-porous surfaces” was performed.

The samples used for the antimicrobial assays included silicone rubber films (SRf), silicone rubber dipped or sprayed with silicone in THF (SR), and silicone samples coated with GNPs. 14 mm sterile commercial tissue culture polyethyleneterephthalate (TCPET) slides were included in the assays as controls for a surface which promotes bacterial adhesion. 9 mm polypropylene (PP) films were used to force contact of the inoculum with the surface. 5 replicas of each sample were used for inoculation and 2 replicas were used as control with no bacteria. All silicone samples were cut into 11 mm disks using a stainless-steel puncher and sterilized using ethylene oxide, available at Hospital de São João. This is a common sterilization method for catheters and other surgical materials. The PP films were cut into 9 mm disks and were sterilized using ethanol for 15 + 15 min, and subsequently washed 3 times with PBS.

A concentrated *S. epidermidis* inoculum obtained from overnight culture in TSB was centrifuged at 2700 rpm for 10 min and subsequently washed 2 times in the same conditions using 5 mL of fresh TSB. The concentration of the inoculum was adjusted to a concentration of 6×10^5 CFU/mL by optical density (OD) reading at 600 nm. The resulting suspension was used to inoculate the surface of the samples with 15 μ L. The sterile PP films were gently placed on top of each sample and light pressing was used so the drop fully spread and covered the area between the sample and the film. The 24-well plates

containing the samples and the controls were then incubated at 37 °C for 24 h in an oven. At least 4 wells were filled with dH₂O to prevent evaporation of the suspension.

A volume of 1 mL of PBS was added immediately after inoculation for 3 replicas of SR and 1.5 mL of TSB was added after the 24 h period for the other samples. This volume was collected and dispensed several times to detach the PP film and the loosely adhered bacteria in the sample. At the first timepoint (t=0 h), the supernatant was used to investigate recovery rate of the bacteria. The supernatant resulting from 24 h incubation was used to investigate antibacterial activity of the samples on non-adherent bacteria. The surface of the sample was also used to measure antibacterial activity of the adherent bacteria. The procedure is illustrated in Figure 8.

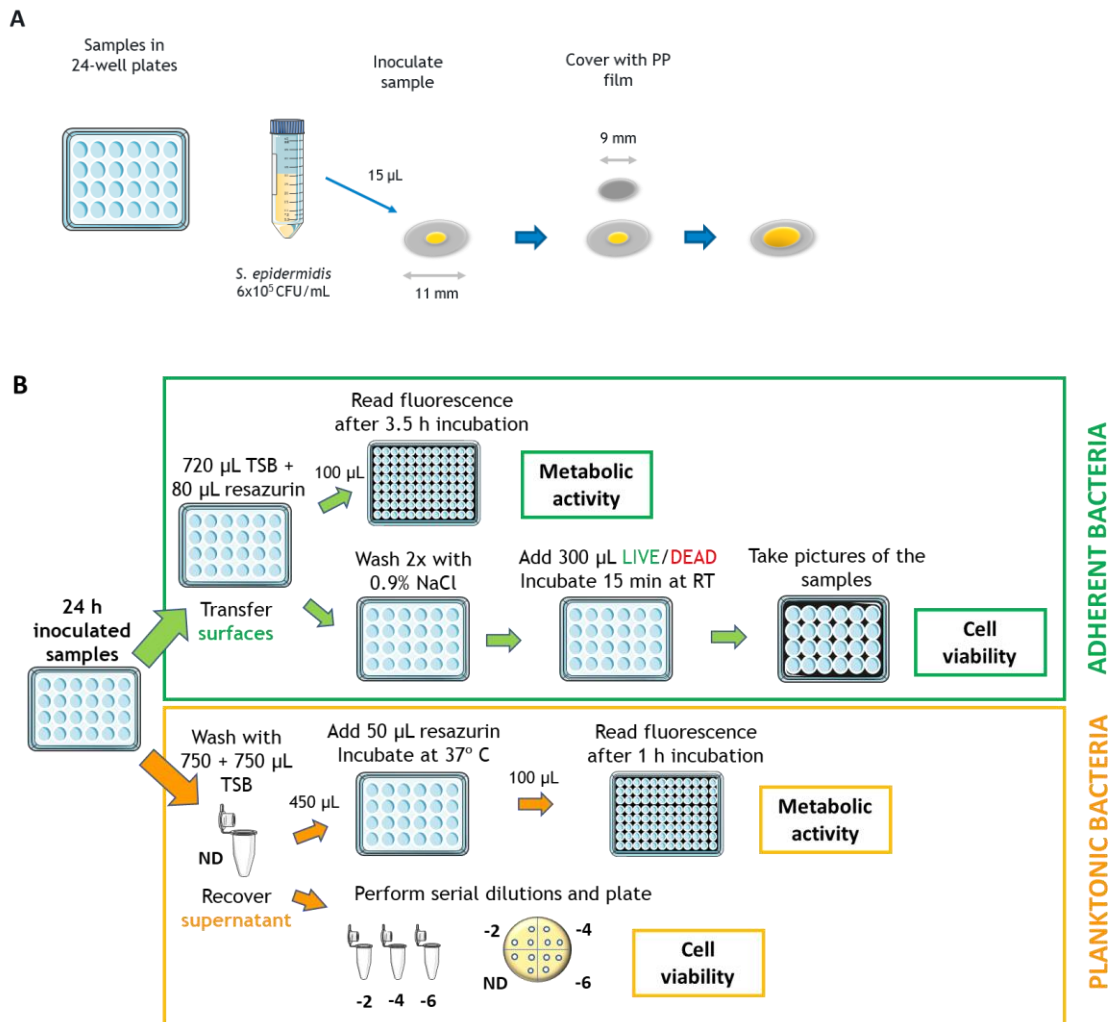


Figure 8. Schematics of the antibacterial assay. (A) Surface inoculation and PP film placement for forcing contact with the inoculum; (B) Testing after 24 h incubation.

3.2.1. Testing in adherent bacteria

All samples were transferred to 24-well plates, previously filled with 720 μL of TSB to perform resazurin assay. Three wells of TSB were used as control. 80 μL of resazurin were added to each well. The plates were incubated at 37°C and 100 μL of each supernatant were transferred to a black-walled 96-well plate after 2h30min and 3h30min of incubation. The relative fluorescence units (RFUs) of the media were measured using a Synergy™ Mx (Biotek, USA) fluorometer (λ_{ex} : 530 nm; λ_{em} : 590 nm), providing indication of the metabolic activity of the bacteria adherent in the surface.

After this assay, the surfaces were washed 2 times with 0.9% NaCl to remove any resazurin stain residues and then stained with BacLight™ LIVE/DEAD® Kit (Molecular Probes, USA) to investigate the viability of the bacteria adhered to the surface. The kit contains a mixture of SYTO9 and propidium iodide (PI) dyes, which stain viable bacteria in green and bacteria with compromised membranes in red, respectively. The staining solution was prepared from stock SYTO9 and PI by diluting the volume of each stain in the same volume of dH_2O . 300 μL of the staining solution were added to each well and kept at room temperature for 15 min. The samples were dried and transferred to a glass bottom 24-well μ -Plate (IBIDI, Germany) with the surface with adherent bacteria facing the glass. Pictures of 30 fields per sample were automatically taken using the IN Cell Analyzer 2000 (GE Healthcare Life Sciences, UK) in the channel with filters for FITC and Cy3. The quantification of bacteria stained with green, red and orange (colocalization of both dyes) in the pictures was performed using the CellProfiler software with a pipeline designed for this purpose. The pipeline automatically detects bacteria from black and white pictures of SYTO9 and PI stainings, based on intensity of staining and size, whose minimum and maximum values were inserted manually. The program outputs a file which counts live bacteria in the FITC channel, dead bacteria in the Cy3 channel, and dying bacteria, which are a colocalization of both stainings recorded on the SYTO9 channel. Any pictures taken out of focus or considered of low quality were discarded. This was performed after the output of the program, by manually analyzing the fields in which the bacteria counted were zero or too high.

3.2.2. Testing in bacteria in suspension

The supernatant obtained from the recovery rate samples was used to perform serial dilutions of 10^{-1} , 10^{-2} , and 10^{-3} (50 μL + 450 μL PBS) to immediately plate in TSA plates. A total of 3 drops of 10 μL for each dilution including non-diluted supernatant were plated and kept in an oven at 37 °C overnight. The colony forming units (CFUs) were then counted.

The recovered supernatant from all the other samples 24 h after incubation was used to perform metabolic activity assay by resazurin assay. 450 μL of non-diluted supernatant was transferred to 24-well plates, followed by the addition of 50 μL of resazurin. TSB was present in 3 wells as the control. The plates were incubated at 37°C and 100 μL of each supernatant were transferred to a black-walled 96-well plate after 30 minutes and 1 hour of incubation, so the relative fluorescence units (RFUs) of the media were measured (λ_{ex} : 530 nm; λ_{em} : 590 nm) using a fluorometer. The RFUs were correlated to the metabolic activity of the bacteria present in the medium.

Serial dilutions were also performed (10^{-2} , 10^{-4} , and 10^{-6}) using TSB as diluting media. 3 drops of 10 μL were plated and kept in an oven at 37 °C overnight and the CFUs were then counted.

4. Statistical analysis

4.1. Contact angles

Statistical analysis for the contact angles measurements were performed with GraphPad Prism 6 using the Kruskal-Wallis test for nonparametric samples ($\alpha=0.05$). The samples of coatings containing GNP-M5 or GNP-M5ox were compared separately.

4.2. Antibacterial assays

Statistical analysis of the CFU counts and total bacteria coating were performed with GraphPad Prism 6 using ordinary one-way ANOVA. Statistically significant differences between silicone and GNP-coated samples are presented in the respective figure. For better visualization of the figures, statistical results regarding TCPET samples are presented in Annex.

Statistical analysis for the measurements of relative fluorescence units was performed with GraphPad Prism 6 using the Kruskal-Wallis test for nonparametric samples ($\alpha=0.05$).



CHAPTER IV: Results and Discussion

1. Graphene nanoplatelets characterization

SEM images of GNP-M5 dry powder and lyophilized GNP-M5ox were analyzed to investigate the morphology of the nanoplatelets (Figure 9A-D).

In GNP-M5 as a dry powder, aggregates of nanoplatelets were predominant (Figure 9A). The aggregates varied in size, and hence in number of aggregated platelets. Aggregation is inevitable due to the high surface energy of the materials and a decent separation is only likely to occur in a well-dispersed solution. However, isolated platelets were still found, as detected in higher magnification images (Figure 9B). The platelets present a planar morphology and sharp edges as documented for non-oxidized materials. The estimated nanoplatelet diameter of 5 μm was also confirmed.

The oxidation of GNP-M5 into GNP-M5ox by Modified Hummers Method (MHM) induced changes in the morphology of the nanoplatelets. Lyophilization of the GNP-M5ox aqueous dispersion resulted on the formation of numerous thin, wrinkled films constituted by fused nanoplatelets (Figure 9C). Higher magnification images show the typical planar, sharp structure was lost and a new wrinkled, folded structure was present instead (Figure 9D).

These changes are described in literature as the ones expected in oxidized GBMs.¹³⁶ Therefore, the oxidation obtained by MHM can be considered successful.

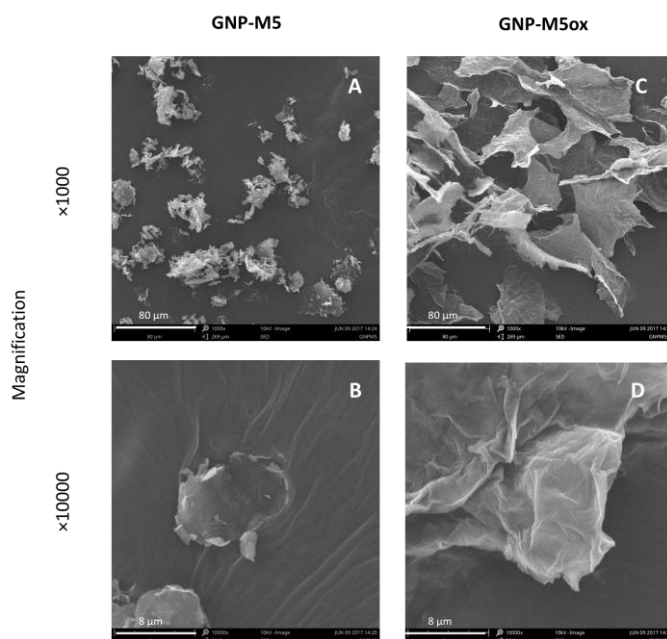


Figure 9. SEM images of the GNP-M5 powder and lyophilized GNP-M5ox. Pictures taken at the magnification of $\times 1000$ and $\times 10000$ (Scale bar = $80 \mu\text{m}$ and $8 \mu\text{m}$, respectively).

XPS analysis provided additional and quantitative information regarding oxidation of GNP-M5 to GNP-M5ox. The atomic composition of the surface is present in Figure 10A. As expected, the percentage of oxygen in GNP-M5ox is much higher than the non-oxidized GNP-M5. The percentage of oxygen is close to 30% is in accordance to what is expected for materials oxidized by MHM.¹³⁷⁻¹³⁹

For non-oxidized GNP-M5, the C1s spectrum presents one large peak, dividable into two peaks (Figure 10B). This pair of peaks at 284.5 eV and 285 eV represent the sp^2 and sp^3 hybridization states of carbon, respectively. Peaks related to the bonds of carbon with oxygen are inexistent or too small to distinguish. A broad tail which spreads towards higher energies (between 289 and 293 eV) is typical of materials with high content in sp^2 carbon.¹⁴⁰ However, for oxidized GNP, the spectra for C1s is very distinct (Figure 10C). Apart from the peak detected in GNP-M5, another large peak and a smaller peak appear. In total and after deconvolution, six different peaks related to different carbon bonds are present. The type and percentage of content for each group are present in Figure 10D. The C sp^2 content decreased relatively to the non-oxidized GNP due to the breaking of C-C sp^2 bonds and formation of new C-C sp^3 bonds and bonds with oxygenated groups.¹³⁷ Peaks corresponding to epoxy groups (C-O-C) are formed due to H_2SO_4 action, and carboxyls (C-OOH) and aldehydes (C=O) are related to the strong oxidizing power of KMnO_4 .¹³⁹

Overall, it is possible to see the peaks related to oxygen-carbon bonds were clearly absent in GNP-M5 spectra. These results prove the oxidation by MHM introduced various types of oxygenated groups.

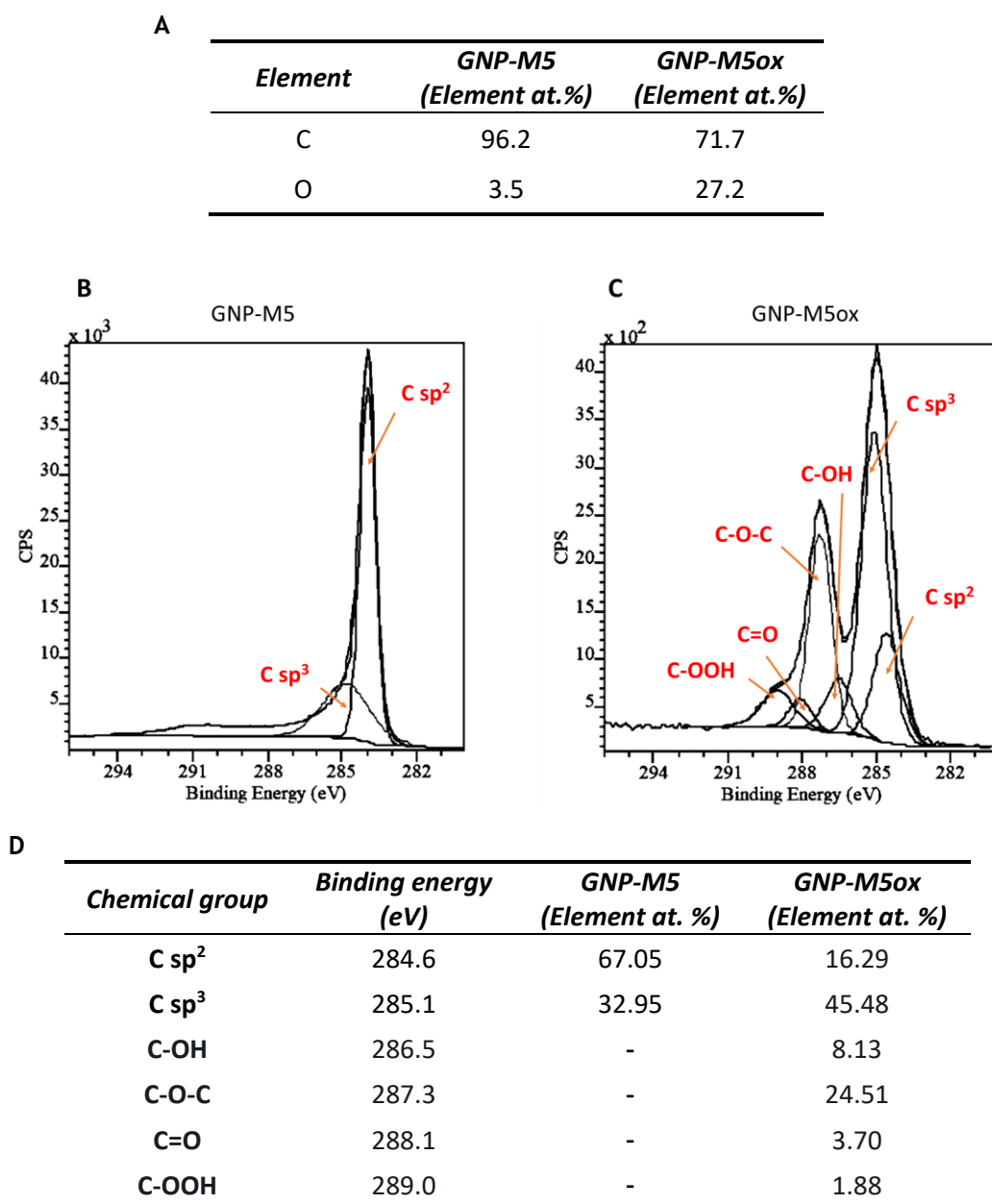


Figure 10. XPS analysis of GNP-M5 and GNP-M5ox. (A) Atomic percentage of carbon and oxygen obtained by analysis of the survey; (B) C1s high-resolution spectrum of GNP-M5; (C) C1s high-resolution spectrum of GNP-M5ox; (D) Contents of chemical groups resulting of C1s spectra fitting.

2. GNP-coated silicone

2.1. Silicone rubber films

Silicone rubber films were characterized in terms of surface and average thickness. As seen from Figures 11A and 11B, the films are transparent and have a smooth surface. From Figure 11C, it is possible to see the thickness was estimated to be of around 300 μm .

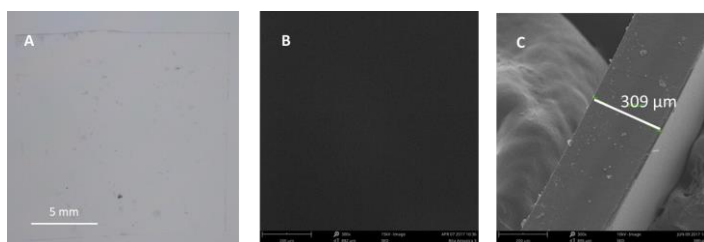


Figure 11. Silicone rubber film. (A) Stereomicroscopy image; (B) SEM image of front view; (C) SEM image of side view. SEM pictures taken at the magnification of $\times 300$. (Scale bar= 200 μm).

2.2. GNP coating with no binder

2.2.1. Dip coating

Dip coating of 1mg/mL GNP-M5 in THF yielded relatively inhomogeneous samples, as can be observed in Figure 12B. The presence of GNP-M5 in the coating changed the overall appearance of the sample from transparent to black, although the coating is far from being opaque.

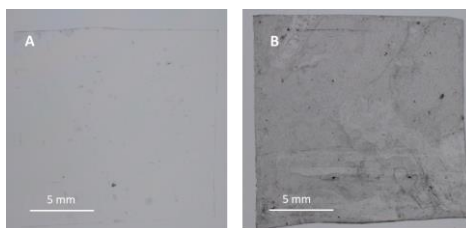


Figure 12. Stereomicroscopy images of (A) silicone base film and (B) 1 mg/mL GNP-M5 in THF dip coating sample (Scale bar=5 mm).

After performing the rubbing test, it was noticeable that the materials were loosely adhered on the surface, as the rubber had detached materials and traces were left on the surface (Table 6). For this reason, no further testing was performed on these samples.

Table 6 - Rubbing test for the dip coatings with no binder. Score of 0 is a clean rubber and 5 is a rubber presenting high GNP detachment.

<i>Condition</i>	<i>GNP concentration</i>	<i>Scale 0 - 5</i>
GNP/THF	1 mg/mL	4

2.2.2 Spray coating

Unlike dip coated samples, THF spray coated samples with no binder produced a homogenous surface (Figure 13). This is explained by the fine atomization of the suspension applied by the aerograph. The sample is yet again black but still translucent.

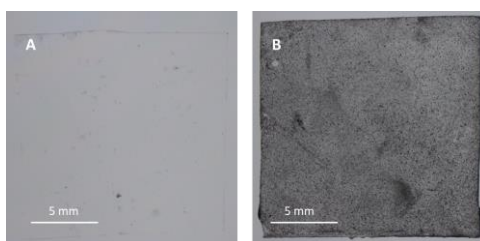


Figure 13. Stereomicroscopy images of (A) silicone base film and (B) 1 mg/mL GNP-M5 in THF spray coating sample (Scale bar=5 mm).

This compromised the adherence of the materials to the surface, and therefore, the results of the rubbing test yielded a black rubber (Table 7).

Spray coating with ethanol yielded a relatively well covered surface, as can be observed in Figure 14, although it was clear the dispersion rolled off easily when sprayed on the vertical silicone surface.

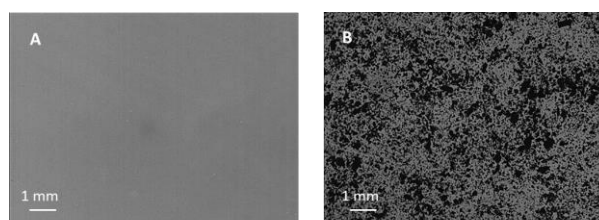


Figure 14. Optical microscopy images of (A) silicone base film and (B) 1 mg/mL GNP-M5 in EtOH spray coating sample (Scale bar=1 mm).

Spray coating samples with THF also did not perform well on the rubbing test. After light rubbing the rubber was black, which indicates loose GNP on the surface (Table 7).

Table 7 - Rubbing test for the spray coatings with no binder. Score of 0 is a clean rubber and 5 is a rubber presenting high GNP detachment.

<i>Condition</i>	<i>GNP concentration</i>	<i>Scale 0 - 5</i>
GNP/EtOH	1 mg/mL	5
GNP/THF		5

Both types of spray coated samples with no binder were discarded for further testing owing to the rubbing test results.

3.1. GNP coating with binder and antimicrobial activity

3.1.1. Dip coating

From observation of Figure 15, the heterogenous appearance of the coatings is clearly noticeable. Frequently large blots of GNP appear because the film tends to curl after the contact with THF. This creates a trapping of the dispersion in some areas of the surface.

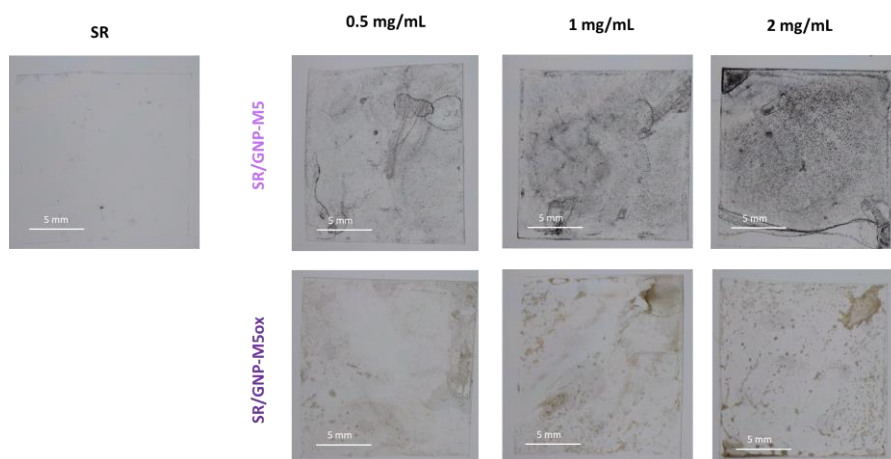


Figure 15. Stereomicroscopy images of SR/GNP dip coating samples (Scale bar = 5mm).

By observation of the SR/GNP-M5 and SR/GNP-M5ox samples in bright field under an optical microscope, it was possible to further investigate the distribution of the GNP across the surface of the sample (Figure 16). Black spots and aggregates of GNP-M5 of varied sizes were easily perceivable and distinct from the rest of the silicone coating. As the light

easily penetrated the sample, the GNP-M5 aggregates present on the back of the sample were also visible as dark blurred spots. The GNP-M5 varied from apparent single platelets to aggregates of 100 to 200 μm in diameter in the lowest concentrations but at 2 mg/mL large aggregates with up to 400 μm appear. Ideally, large aggregates would be separated in the ultrasonication process. Yet, some aggregates always appear in solution due to the high surface energy of the GBMs. As the concentration of GNP used in dip coating grows, a larger area of the surface tends to be more covered with GNP. In the lowest concentration, large aggregates appear isolated, having mostly silicone in spaces between. The distribution of GNP-M5ox differed from that of GNP-M5. The agglomerates of particles forming a dotted pattern were homogenous in size and distribution. These aggregates were now brown instead of black due to the brownish color already detected in the oxidation of the GNP. The area of surface covered, however, was similar to the GNP-M5 dip coated samples.

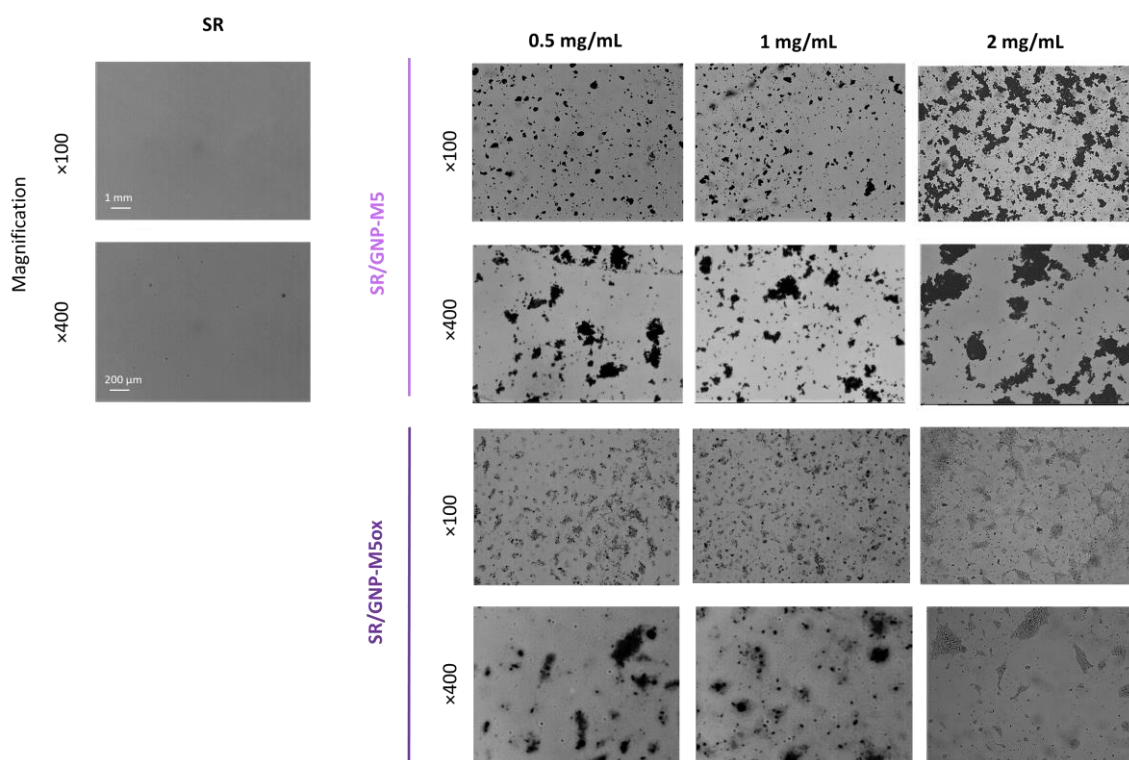


Figure 16. Optical microscopy images of SR/GNP dip coating samples. Pictures taken at the magnification of $\times 100$ and $\times 400$ (Scale bar=1 mm and 200 μm , respectively).

Overall, it is possible to conclude that the dip coating technique presents GNP at the surface, but a great area is still left devoid of GNPs.

The rubbing and washing test made it possible to understand if the platelets were well adhered to the coating. Rubbing on any of the SR/GNP-M5 samples did not leave any black traces on the rubber (Table 8). The water from the washing test was seemingly clear in all dip coated samples, except for a few aggregates in suspension for the concentration of 2 mg/mL in SR/GNP-M5 samples. Nevertheless, it is likely that the vast majority of the GNP on the surface is very well adhered, as the forces of the vortex water are harsher than a normal catheter surface would experience from contact with blood flow (Figure A1). The silicone thin film deposited along with the GNP may be contributing for the bonding of the latter to the surface of the base film.

Table 8 - Rubbing test for the SR/GNP dip coating samples. Score of 0 is a clean rubber and 5 is a rubber presenting high GNP detachment.

Concentration (mg/mL)	Scale 0 - 5	
	SR/GNP-M5	SR/GNP-M5ox
0.5	0	0
1	0	0
2	0	0

The distribution of GNP on the surface was further investigated by SEM (Figure 17). The presence of aggregates of GNP-M5 of different sizes as detected on optical microscopy images was confirmed. Furthermore, it is possible to see that these aggregates are quite covered or surrounded by polymer and only a part of the GNP is exposed. In some cases, only the edges are protruding while the rest of the nanoplatelet is lying flat, partially covered by silicone. SR/GNP-M5ox coated samples, in contrast, present no aggregates and few isolated nanoplatelets on the surface. Instead, frequent creased structures made up of wrinkled GNP-M5ox sheets entrapped in a silicone matrix appear. This behavior is expected, as oxidized sheets tend to stick together. The presence of silicone in the coating may be facilitating the interconnection of the platelets.

In general, SEM images display less GNP than expected by analyzing bright field images. This can be explained by the coverage of some agglomerates by the polymer, which is transparent to light but is opaque to electrons. For this reason, a silicone to GNP proportion of 1:2 was tested (Figure A2). The surface did not present significant improvements in GNP exposure.

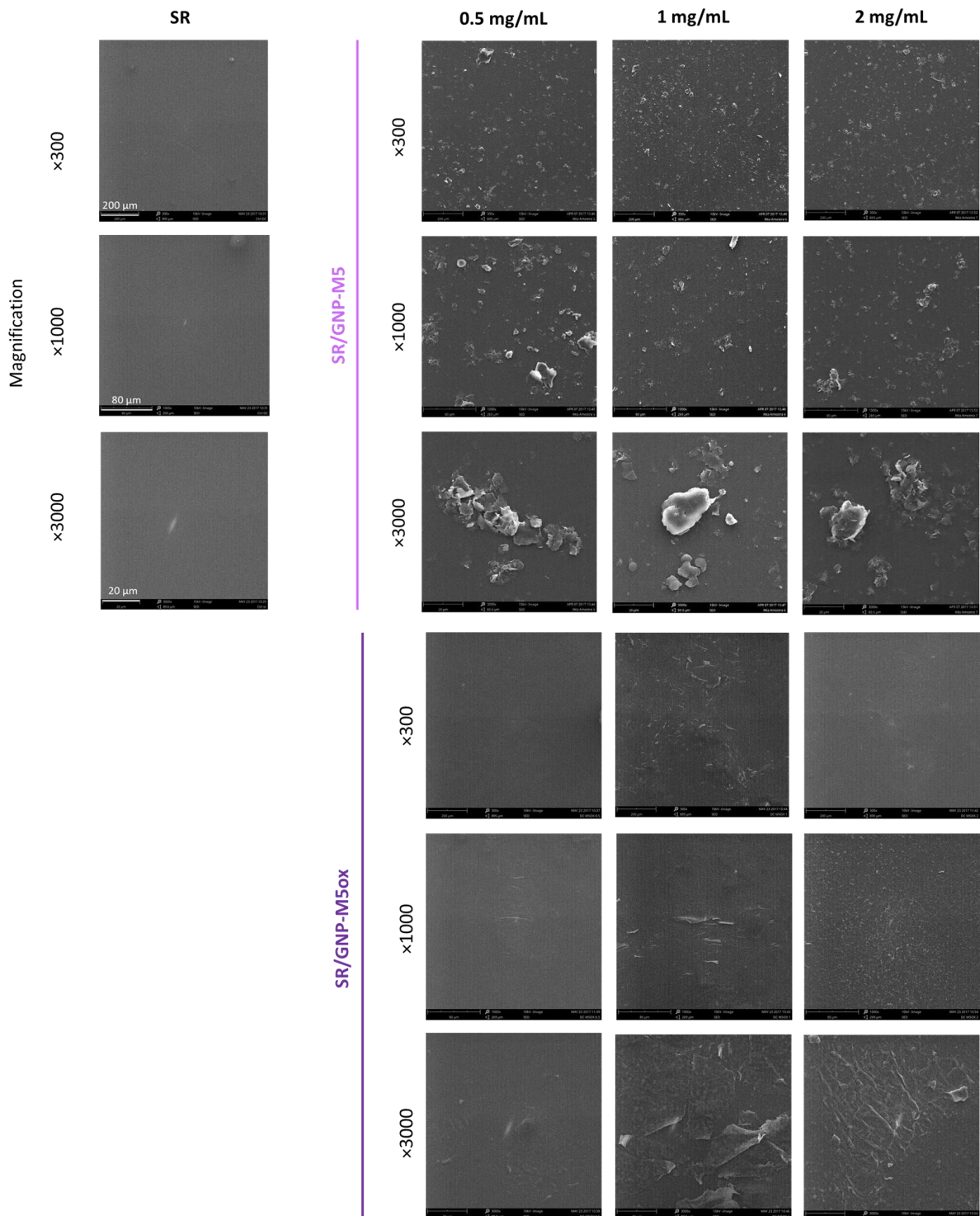


Figure 17. SEM images of SR/GNP dip coating samples. Pictures taken at the magnifications of $\times 300$, $\times 1000$ and $\times 3000$ (Scale bar= 200 μm , 80 μm and 20 μm , respectively).

The water contact angle was measured to investigate the wettability of the samples (Figure 18). The contact angle of silicone film (SRf) is in accordance to the literature for PDMS (117°).¹⁴¹ SR/GNP-M5 coated samples exhibited a slight trend in increasing in the contact angle with the increasing concentration of GNP. On one hand, the existence of platelets at the surface might add to the roughness effect which increases the contact angle. On other hand, the non-oxidized GNP is itself hydrophobic as its made up of elemental carbon. Dip coating with SR/GNP-M5ox produced the contrary result, as the contact angle is tending to decrease relatively to SR, with a similar value in all concentrations. This is a result of the introduction of the oxidized, hydrophilic GNP which contains numerous oxygenated groups that form hydrogen bonds with water.

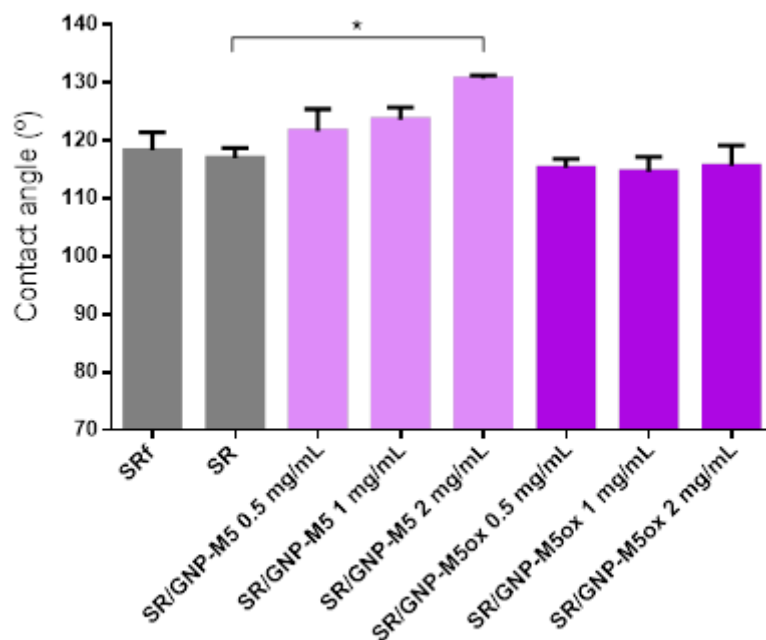


Figure 18. Water contact angle for SR/GNP dip coating samples. Statistical analysis performed by Kruskal Wallis test and statistically significant differences are indicated with * ($p \leq 0.05$).

In sum, the dip coating technique provided GNP exposure, while efficiently attaching the clear majority materials on the surface, as confirmed by the rubbing and washing tests. The coating produced on the surface is close to being a nanocomposite constituted of GNP and silicone, although the GNPs are in low concentrations. To perform antibacterial activity tests, and due to time constraints, the concentrations of 1 mg/mL and 2 mg/mL were selected. The choice was mainly based on the difference recorded in contact angle in the two mentioned concentrations, and on the slight differences noticed in GNPs exposure by SEM.

Dip coating samples of GNP-M5 and GNP-M5ox with the concentrations of 1 mg/mL and 2 mg/mL were evaluated in terms of antibacterial activity. With this aim, the cell viability and metabolic activity of the bacteria in the supernatant (planktonic bacteria) and on the surface (adherent bacteria) were investigated.

From observation of Figure 19A, it is possible to see that there are always metabolically active bacteria on the surface of silicone and SR/GNP samples. Regarding the total number of adherent bacteria/mm², values are higher for the 2 mg/mL concentration for both SR/GNP-M5 and SR/GNP-M5ox coatings than what was observed for silicone samples (Figure 19B and 19D). The samples of concentration of 1 mg/mL had a quantity of bacterial adhesion similar to silicone samples. The percentage of dead bacteria for silicone samples is never higher than 40%, although the quantity dying bacteria stained in orange is higher than for SR/GNP samples (Figure 19C). These samples present 184 live bacteria/mm². However, it is possible to see that for 1 mg/mL samples, SR/GNP-M5 presented 38% of dead bacteria, while the oxidized coating had 71% of bacterial death, yielding 79 and 51 live bacteria/mm² respectively. For the 2 mg/mL concentration, in SR/GNP-M5ox samples 85% of the bacteria are dead, while for SR/GNP-M5 the percentage of dead bacteria is only of 50%, yielding 93 and 321 live bacteria/mm², respectively. The increased number in SR/GNP-M5 2 mg/mL samples and 50% of viability explains why the metabolic activity for this samples is slightly higher. Bacteria were seen attached to GNP aggregates, and many of them were dead close to the edges of GNP-M5 but for GNP-M5ox there appears to be no difference for edges or basal planes (Figure 19E). For TCPET samples, the percentage of dead bacteria was very low. Although the number of adhered bacteria was similar to silicone samples, no notorious differences were seen on the metabolic activity assay.

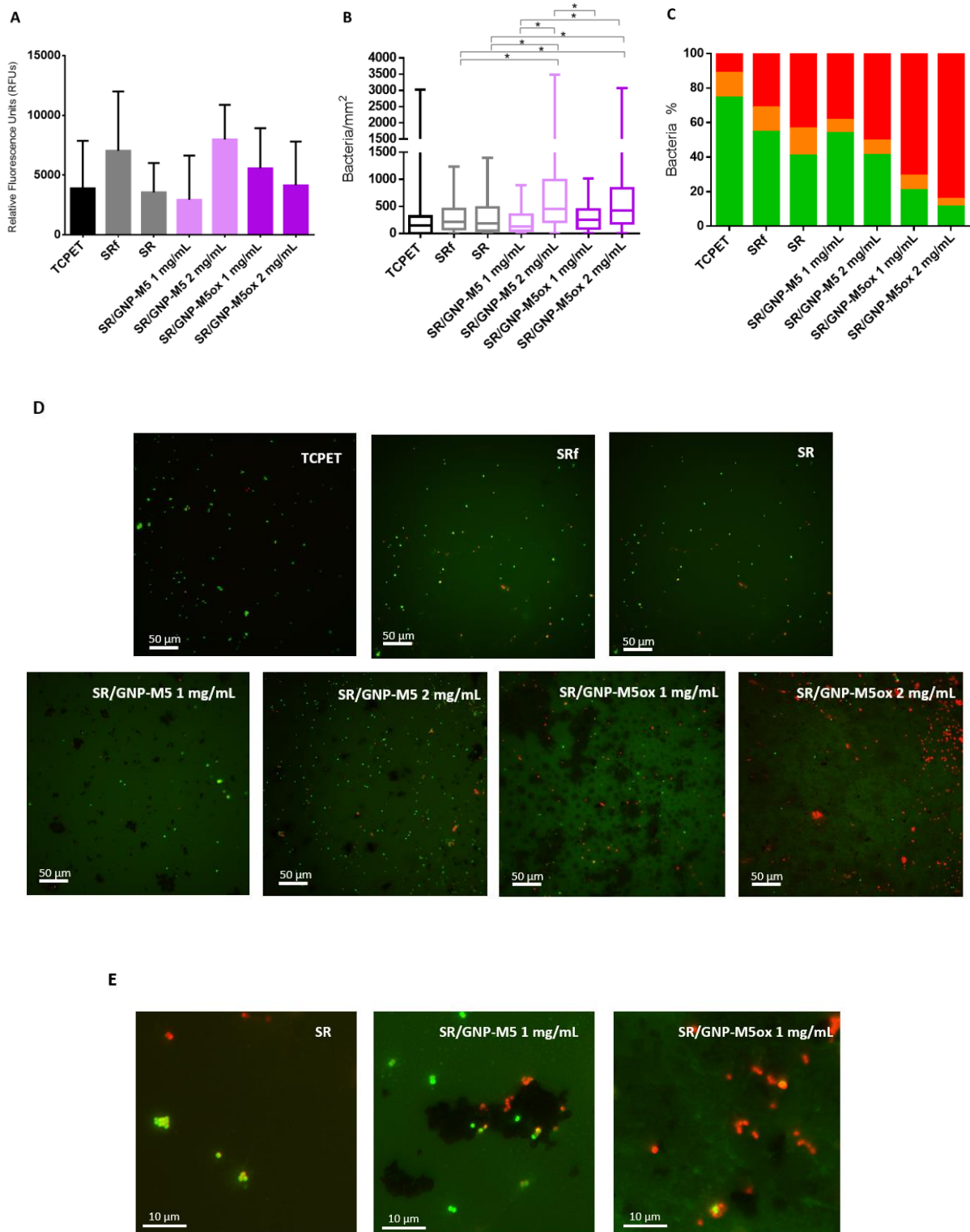


Figure 19. *S. epidermidis* adherent to SR/GNP dip coating samples after 24 h incubation. (A) Metabolic activity of bacteria in the surface after 3,5 hours incubation with resazurin; (B) Total adhered bacteria per mm^2 ; (C) Percentage of live (green), dying (orange) and dead (red) bacteria; (D) Representative images of the LIVE/DEAD staining (Scale bar= $50\ \mu\text{m}$); (E) Images of bacteria adhered to SR and GNP aggregates (Scale bar= $10\ \mu\text{m}$). Statistical analysis of the metabolic activity assay and total adhered bacteria performed with Kruskal-Wallis test and ordinary One-way ANOVA, respectively. Statistically significant differences are indicated with * ($p \leq 0.05$).

The recovery rate for the SR samples was of 86% (Table A2). Therefore, it is possible to conclude that the majority of bacteria are recovered in suspension. For planktonic bacteria, after one hour of incubation, the fluorescence of the supernatant was measured. As Figure 20A depicts, none of the dip coated samples reduced the metabolic activity of the collected bacteria. No statistically significant differences were observed between any group. Furthermore, no sample inhibited the growth and viability of bacteria. From Figure 20B it is possible to understand that the bacteria divided and greatly increased in number from the initial inoculum of 10^5 CFU/mL. TCPET and the GNP-M5 group were the most effective in controlling bacteria growth, when comparing to the SR control and with GNP-M5ox samples. Figure 20A and 20B together suggest that TCPET and GNP-M5 samples present bacteria that although viable, are non-cultivable.

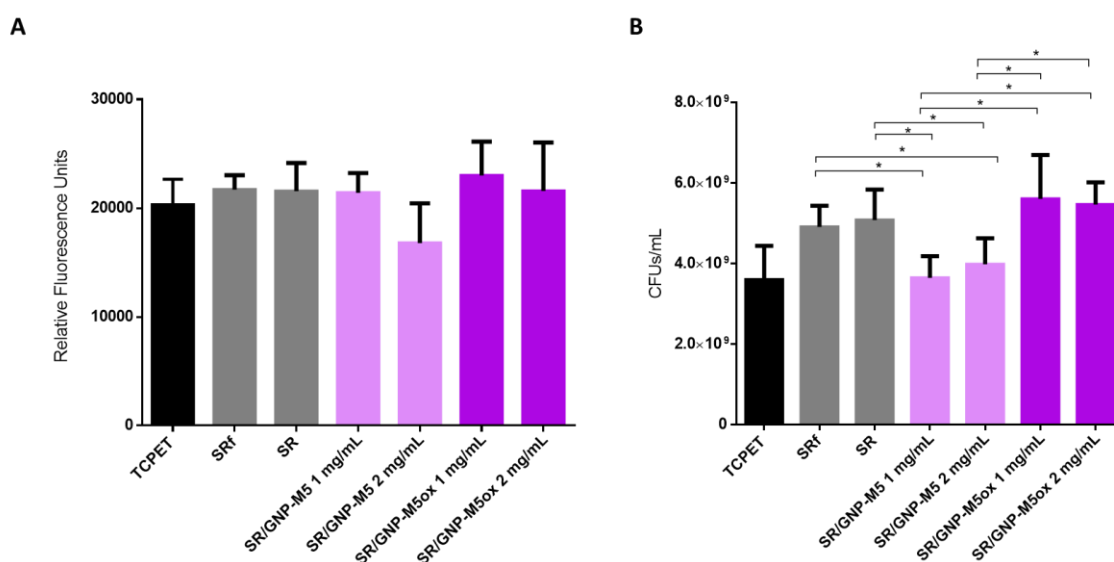


Figure 20. Planktonic *S.epidermidis* of SR/GNP dip coating samples after 24 h incubation. (A) Metabolic activity of bacteria in suspension after 1 hour incubation with resazurin and (B) colony forming units of the viable bacteria collected in supernatant. Statistical analysis of metabolic activity was performed with Kruskal-Wallis test and CFUs with ordinary One-way ANOVA. Statistically significant differences are indicated with * ($p \leq 0.05$).

Overall, it is possible to see that SR/GNP-M5ox coatings were more effective in killing bacteria than SR/GNP-M5 coatings, especially for the 2 mg/mL concentration. At this concentration, independently of the GNP considered, the ratio of antimicrobial activity is at least 1.6 times better than the 1 mg/mL samples and the SR samples. Nevertheless, many bacteria are attracted to the surface. Even if they are in fact dead, this could be a negative aspect because their presence may contribute to the formation of biofilm.¹⁴² This is why the SR/GNP-M5ox at 1 mg/mL would be the best condition for dip coating antimicrobial samples, as it kills bacteria but restricts their attachment.

According to work of Santos, *et al*⁹⁶ the inclusion of GO in a polymer composite coating enhanced its antimicrobial activity when compared to the activity of GO coating alone. This is explained by the improved dispersibility of the material in the polymer matrix. As the dip coating technique appears to have produced a thin nanocomposite film of GNPs and silicone at the surface of the silicone base film, a similar process may be happening. Still, a lower percentage of dead bacteria in SR/GNP-M5 coatings when compared to SR/GNP-M5ox coatings could be derived from the surface topography.

3.2.2. Spray coating

The GNP-M5 dispersion applied by spray coating deposited a high amount of GNP on the surface of the samples as seen on Figure 21. An increase in the concentration of GNP used resulted in an increase in the covered area of the sample. At the concentration of 2 mg/mL the samples are almost opaque. Additionally, and much like spray coated samples with no binder, the distribution of the GNPs is very homogenous.

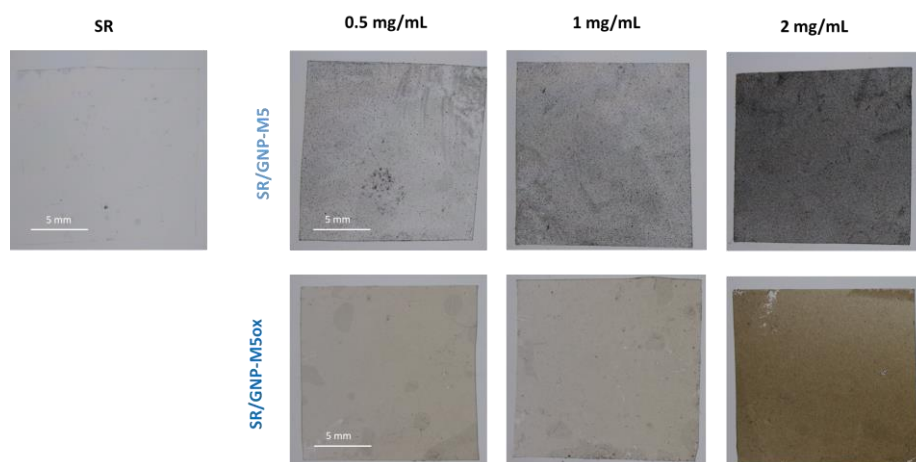


Figure 21. Stereomicroscopy images of SR/GNP spray coating samples (Scale bar = 5mm).

By looking at optical microscopy images it is possible to see that although the distribution and size of the GNP-M5 aggregates is considerably homogenous in all samples, for the concentrations of 1 and 2 mg/mL the aggregates increase in size when compared to 0.5 mg/mL and with dip coated samples (Figure 22). These results can be explained by the large amount of dispersion used and the spraying method itself which may create overlapping layers of GNP. Consequently, the areas of silicone without GNP are also much less when compared to dip coated samples. For GNP-M5ox samples, no large agglomerates were present; instead, a pattern of small-sized materials was distributed homogeneously

throughout the samples. An increase in concentration also produced an extended coverage of the surface and hence an increase in the opaqueness of the latter.

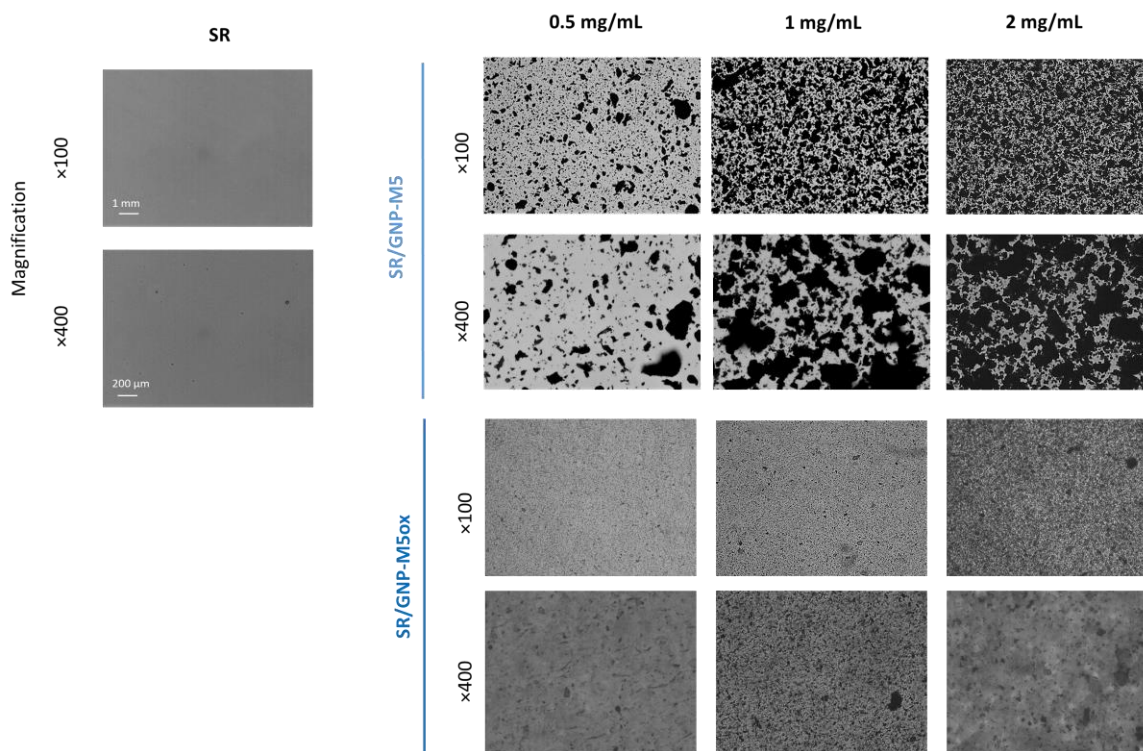


Figure 22. Optical microscopy images of SR/GNP spray coating samples. Pictures taken at the magnification of $\times 100$ and $\times 400$ (Scale bar = $100 \mu\text{m}$ and $20 \mu\text{m}$, respectively).

Because of the various layers coated on the sample, all SR/GNP-M5 samples left traces of detached GNP on the rubbing test (Table 9). It is possible that the silicone in the dispersion is not sufficient to hold in place all the material, in particular for higher concentrations of GNP-M5, where the rubber presented highest detachment. Contrarily, SR/GNP-M5ox samples did not leave any traces of loose materials on the rubber. It is therefore likely that the sprayed coating is cohesive and uniform. All GNP-M5 samples resisted the washing test but the coatings on SR/GNP-M5ox samples were compromised, especially on the 2 mg/mL concentration. The coating partially detached from the edges of the square film and totally detached from the area where the tweezers held the sample. However, both coatings appeared with normal morphology in SEM images (Figure A3). Nevertheless, these results suggest once again that the silicone in the coating is sufficient to act as a glue to hold the materials together but partially fails to promote the adhesion to the base silicone film when the GNP concentration is high.

Table 9 - Rubbing test for the SR/GNP spray coating samples. Score of 0 is a clean rubber and 5 is a rubber presenting high GNP detachment.

Concentration (mg/mL)	<i>Scale 0 - 5</i>	
	SR/GNP-M5	SR/GNP-M5ox
0.5	1	0
1	3	0
2	5	1

The abundant coverage of the surface was confirmed by SEM images presented on Figure 23. The increase of coverage with concentration seen on bright field images was also noticeable. The GNP-M5 platelets and aggregates are mainly seen laying on the surface, although some are seen vertically disposed. Little or no polymer appears to be covering the surface of the platelets contrarily to dip coated samples. SR/GNP-M5ox spray coated samples, however, displayed a uniform coating with small nanoplatelets appearing isolated. Apparently, all silicone of the base film is covered by the SR/GNP-M5ox coating. Again, similarly to dip coated samples, wrinkle-like structures are noticeable. In high magnification images, it is possible to see that nanoplatelets are as if fused together, creating a uniform assembly, and their edges are sometimes protruding, forming the wrinkles on the surface.

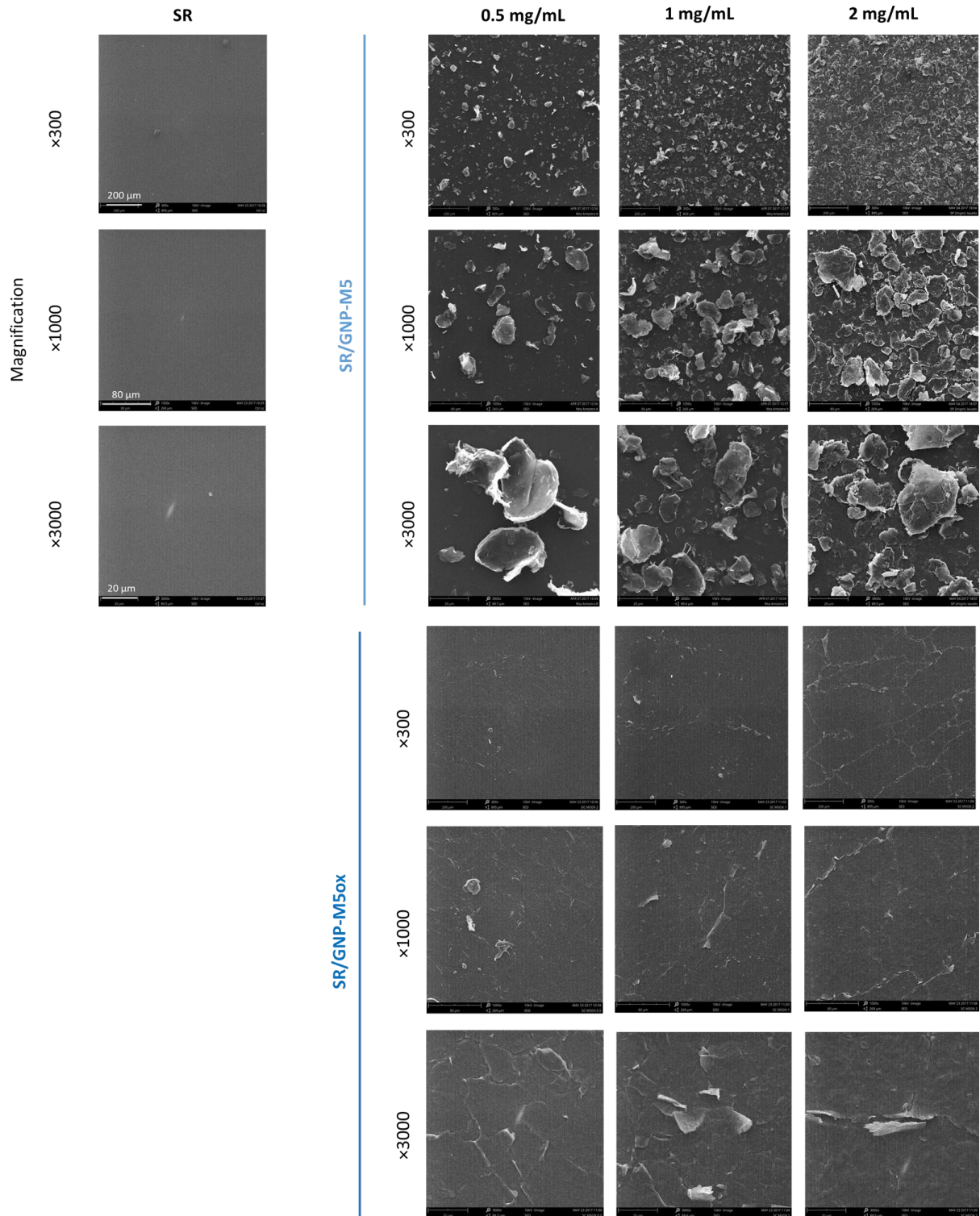


Figure 23. SEM images of SR/GNP spray coating samples. Pictures taken at the magnifications of ×300, ×1000 and ×3000 (Scale bar= 200 μm, 80 μm and 20 μm, respectively).

The water contact angle results for the spray coated samples are displayed in Figure 24. The SRf samples are similar to the SR dip coating control. There is a considerable increase of hydrophobicity in SR/GNP-M5 samples. For the 2 mg/mL concentration the droplet did not stick easily onto the surface (Figure A3). Nevertheless, it was possible to conclude that as the contact angle is superior to 150° the sample may be superhydrophobic¹⁴³ although the high disposition of nanoplatelets can create a very rough surface and induce higher contact angle. In contrast, GNP-M5ox spray coated samples with the two lowest concentrations displayed a smaller contact angle. The presence of oxygenated groups is likely to be causing this effect. However, in the 2 mg/mL samples, the contact angle increased significantly. Once more the roughness of the surface may be playing an important part in the hydrophobicity of the samples in this concentration.

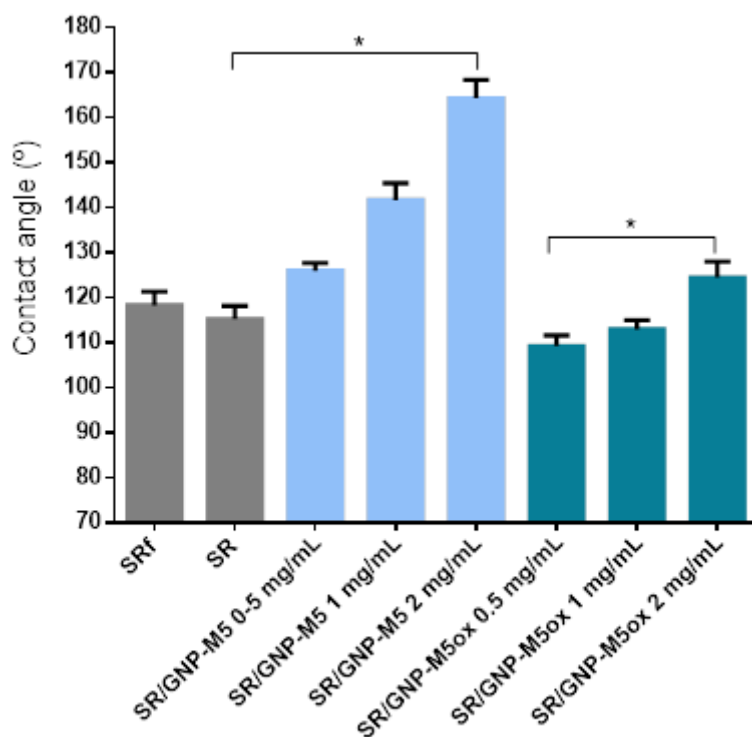


Figure 24. Water contact angle for SR/GNP spray coating samples. Statistical analysis performed by Kruskal Wallis test and statistically significant differences are indicated with * ($p \leq 0.05$).

Overall, the spray coating method provided a great surface exposure of both types of GBMs. The rubbing test suggests SR/GNP-M5 coating is not as cohesive and unified as the SR/GNP-M5ox coating, but the washing test and the contact angle results indicate that the SR/GNP-M5 samples resist better to contact with liquids, contrarily to SR/GNP-M5ox samples.

Because 2 mg/mL samples of SR/GNP-M5 and SR/GNP-M5ox performed the worst on the rubbing and washing test, respectively, the concentrations of 0.5 and 1 mg/mL were used to perform antibacterial activity assays.

From Figure 25A, it is possible to see that SR/GNP-M5 samples present high metabolic activity at the surface. The control material and the silicone samples registered no metabolic activity. Much like dip coating samples, the higher concentration tested also induced more bacterial attachment than the lowest concentration, independently of the GNP considered (Figure 25B and 25D). Still, the 0.5 mg/mL concentration induced more bacterial adhesion than the silicone samples and the control materials. The percentage of dead bacteria was of 27% and 34% for SRf and SR samples - a proportion in all like the SR/GNP-M5 samples which presented 30% and 31% for 1 mg/mL and 2 mg/mL, respectively (Figure 25C). These samples yielded 44 to 87 live bacteria/mm². However, because around 40% of bacteria are alive and many bacteria are attached, this might explain why the metabolic activity is so high for SR/GNP-M5 samples. For GNP-M5ox samples, the percentage of dead bacteria were 64% for 0.5 mg/mL and 47% for 1 mg/mL, yielding 83 and 370 live bacteria/mm², respectively. It is surprising to see an increase in viability with concentration for this samples. It is possible that at this concentration, the coating is starting to become more dense and compact. Generally, bacteria were seen attached to GNP aggregates, and many of them were dead close to the edges of GNP-M5 and throughout GNP-M5ox with no preference for edges (Figure 25E).

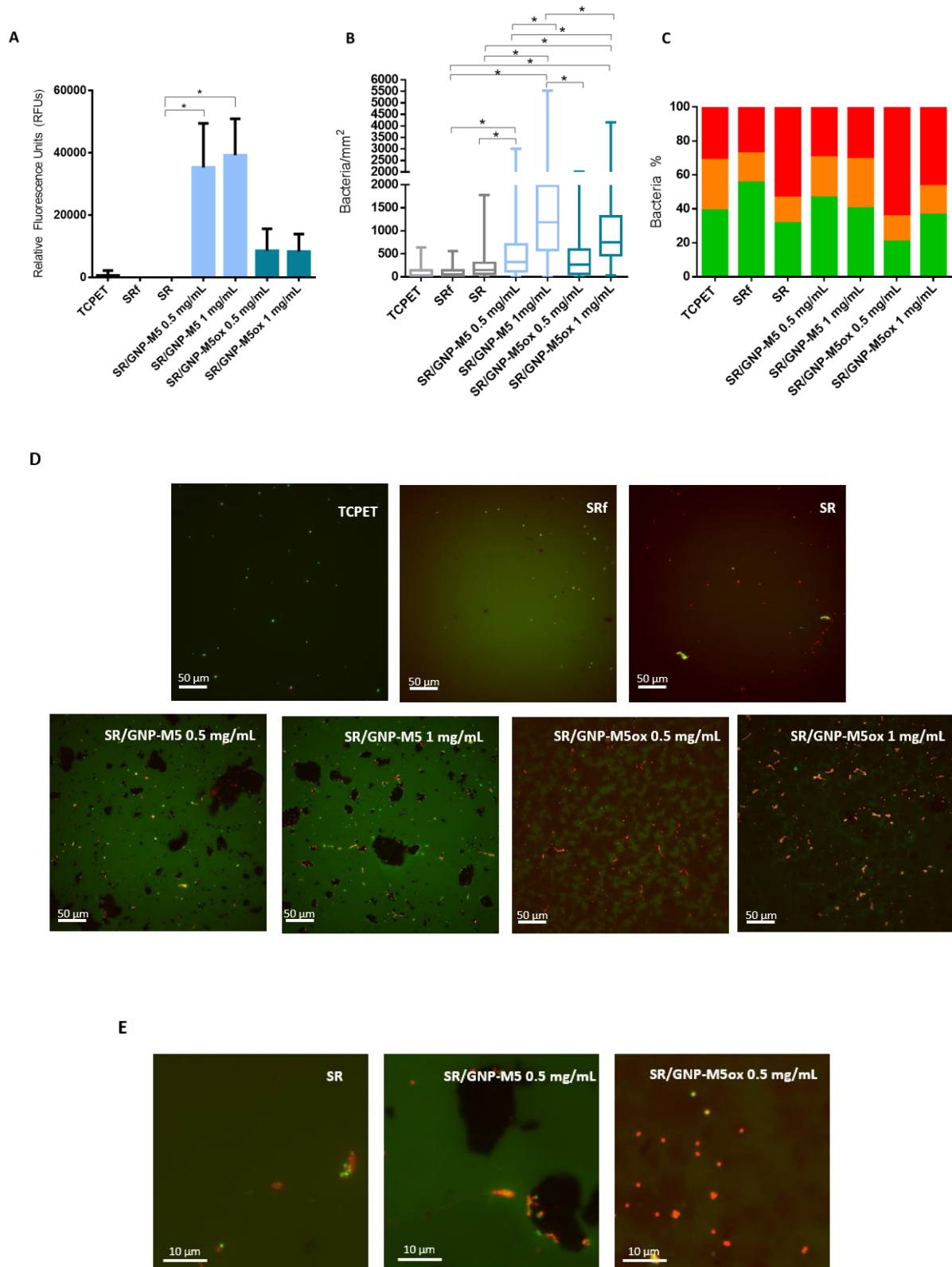


Figure 25. *S.epidermidis* adherent to SR/GNP spray coating samples after 24 h incubation. (A) Metabolic activity of bacteria in the surface after 3,5 hours incubation with resazurin; (B) Total adhered bacteria per mm²; (C) Percentage of live (green), dying (orange) and dead (red) bacteria. (D) Representative images of the LIVE/DEAD staining (Scale bar=50 µm); (E) Images of bacteria adhered to SR and GNP aggregates. (Scale bar=10 µm) Statistical analysis of metabolic activity assay and total adhered bacteria performed with Kruskal-Wallis test and one-way ANOVA, respectively. Statistically significant differences are indicated with * ($p \leq 0.05$).

While the adherent bacteria appeared to be very metabolically active in the surface, for planktonic bacteria there is enhanced activity for the SR/GNP-M5ox samples when compared to SR/GNP-M5 and silicone samples (Figure 26A). The counting of the CFUs confirm this behavior (Figure 26B). Again, like with dip coating samples, no SR/GNP coating restricted bacterial growth and multiplication. The recovery rate calculated for this assay was of 96% (Table A5).

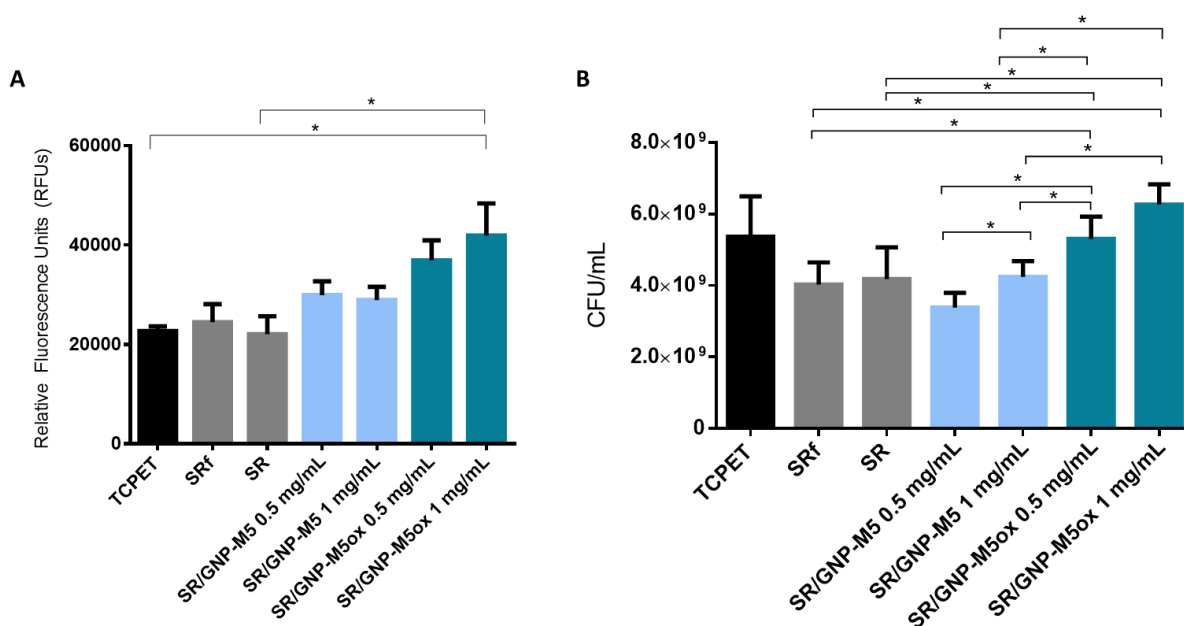


Figure 26. Planktonic *S. epidermidis* of SR/GNP spray coating samples after 24 h incubation. (A) Metabolic activity of bacteria in suspension after 1 hour incubation with resazurin and (B) colony forming units of the viable bacteria collected in supernatant. Statistical analysis of metabolic activity was performed with Kruskal-Wallis test and CFUs with ordinary One-way ANOVA. Statistically significant differences are indicated with * ($p \leq 0.05$).

In sum, spray coating samples appear to promote a very high bacterial adhesion to the surface. This may mean that bacteria have an affinity to GNP aggregates, where they can easily attach, contrarily to the smooth silicone surface. For SR/GNP-M5 samples, because the surface is very rough and the platelets are very exposed, there can be a favorable environment for bacteria to stick to and colonize. There is also a clear effect of the hydrophilicity on adhesion, as the analysis of the supernatant shows. Less hydrophobic surfaces resist bacterial adhesion while hydrophobic surfaces tend to attract bacteria. This is why the metabolic activity was higher in supernatant for GNP-M5ox coatings and higher in the surface for GNP-M5 coatings. Still, SR/GNP-M5ox coatings are better at killing

bacteria than SR/GNP-M5 coatings. In this case, the 0.5 mg/mL concentration produced the best result in terms of antibacterial properties although the quantity of bacteria attachment is still higher than the ideal.

Spray coating with non-oxidized materials, even with silicone present as a binder, yielded loosely attached layers of GNP-M5. The nanoplatelets are mostly found horizontally displayed, therefore bacteria mainly interact with their basal planes. Various authors including Parra, *et al*⁹² defend that graphene coatings with no sharp edges exposed have no significant bacterial activity. Szunerits, *et al*⁸⁷ even reports these coatings promote *E.coli* growth, with no membrane damage being observed. Although SR/GNP-M5ox coating possesses a distinct coating morphology, the basal planes are still what is in contact with bacteria. However, Zhao, *et al*⁹⁸ described the antibacterial activity of a GO coating possibly deriving from the contact with basal planes. Kim, *et al*¹⁴⁴ also defend this theory, stating that charge transfer was the main mechanism involved in membrane stress when GO was coated with basal planes exposed. Therefore, it is possible that the difference in bactericidal activity of the spray coatings is mainly due to the oxidation of the materials.

Overall, spray coating produced different outcomes when compared to dip coating. Because the morphology of the coatings is different, so is their antibacterial activity. On one hand, dip coating samples have much more silicone exposed than spray coating samples, for the same GNP concentration tested. This appears to influence bacterial viability, as they have a less rough surface to stick to and proliferate. On the other hand, the orientation of the platelets is different, especially when looking at GNP-M5 coatings. Yet, the oxidation of the GNP-M5 positively affected the antimicrobial activities for both types of coating, promoting bacterial death. These results are summarized on Figure 27.

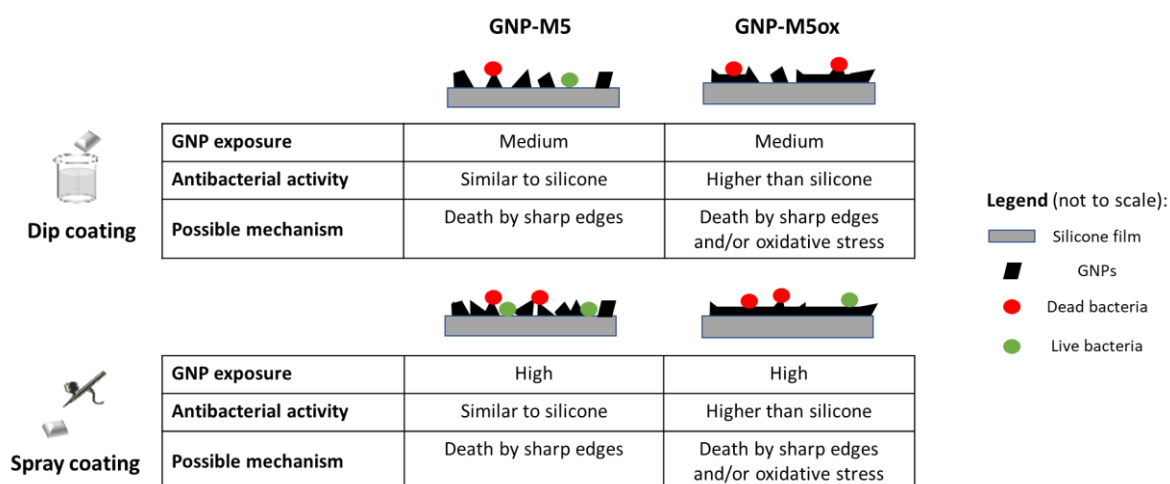


Figure 27. Summary of obtained results.

CHAPTER V: Conclusion and Future Work

1. Conclusion

The oxidation of GNP-M5 to GNP-M5ox changed the morphology of the platelets to a more wrinkled and folded structure. The introduction of different oxygenated groups was confirmed.

Coating GNPs on silicone rubber for antimicrobial purposes was performed for the first time by two different strategies, namely dip coating and spray coating. The presence of a binder in the coatings (silicone) was found to be essential to immobilize the materials on the surface.

Dip coating produced samples with low homogeneity of GNPs on the surface and the overall area of GNP that coated the surface was low, as they presented a great area devoid of GNPs. Furthermore, the GNPs on the surface appeared to be totally or partially masked by the polymer, as some aggregates or edges appeared only somewhat protruding on the surface. However, all coatings had the GNP efficiently immobilized on the surface, as no materials were found in the rubbing and washing tests. Antibacterial testing showed antimicrobial activity for dip coating samples, especially for the coatings with oxidized GNP.

Spray coating yielded very homogenous samples with a full coverage of GNPs on the surface of the silicone. The GNP-M5 platelets were found lying flat on the surface, while GNP-M5ox platelets were found as part of a cohesive coating with few edges protruding from the samples. Because SR/GNP-M5 coatings were not cohesive, materials were detached from the surface with the rubbing test. Notorious differences in wettability were noticed. Spray coating with non-oxidized materials yielded a seemingly superhydrophobic surface while spraying oxidized materials turned the surface more hydrophilic. This impacted the antimicrobial activity, as more bacteria attached to hydrophobic samples. Nonetheless, all coatings attracted a high quantity of bacteria. SR/GNP-M5ox coatings also demonstrated the best results for antibacterial activity, although dip coating still produced better results in terms of lower attachment of bacteria and higher percentage of death.

Globally this work demonstrates the potential of GNP incorporation at the surface of silicone for antimicrobial purposes, although further testing is needed to confirm said properties.

2. Future Work

Although this work answers some questions regarding GNP exposure and oxidation on the antibacterial activity of the coatings, some work is still left to be performed.

Acquiring additional information regarding the surfaces tested with bacteria, namely SEM and/or TEM pictures, could elucidate if the materials are provoking membrane damage.

The measurement of the roughness of the surfaces for all coated samples would be interesting to fully understand if this is a critical factor in bacterial adherence. Furthermore, some testing should be done to confirm if the surface has any traces of solvent which can be contributing to antimicrobial activity in an undesired way. Mechanical testing should also be performed to assess if the coating is altering the silicone base physical properties. Ideally, they should not be altered. Concerning dip coating samples, it should be tested if increasing the number or the time of dip until the surface resembles a spray coating surface have enhanced or hindered effects on the antibacterial activity. Regarding spray coating samples, testing for superhydrophobic surfaces would be interesting to perform under dynamic flow conditions.

Apart from improving and confirming what was already performed, other materials, namely GNP with different diameters could be tested to see if the size of the nanoplatelets has influence in the antimicrobial activity. Also, other types of coating techniques, such as spin coating, could be an alternate approach to exposing GNPs. Furthermore, other bacteria strains that colonize catheters, like *Escherichia coli* and *Staphylococcus aureus*, should be used to validate the antibacterial properties in Gram-negative and Gram-positive bacteria.

References

1. Thomas, J. R. The use of Polymers In {IV} Catheters: Structure, Properties, and Future Developments. *J. Vasc. Access Devices* **7**, 25-33 (2002).
2. Rahimi, A. & Mashak, A. Review on rubbers in medicine: natural, silicone and polyurethane rubbers. *Plast. Rubber Compos.* **42**, 223-230 (2013).
3. Colas, A. & Curtis, J. in *Biomaterials Science (Third Edition)* (eds. Ratner, B. D., Hoffman, A. S., Schoen, F. J. & Lemons, J. E.) 82-91 (Academic Press, 2013). doi:http://dx.doi.org/10.1016/B978-0-08-087780-8.00010-3
4. Jones, R. G., Ando, W. & Chojnowski, J. *Silicon-Containing Polymers: The Science and Technology of Their Synthesis and Applications*. (Springer Netherlands, 2013).
5. Marciniec, B. & Chojnowski, J. *Progress in Organosilicon Chemistry*. (Gordon and Breach Science Publishers, 1995).
6. Dumitriu, S. *Polymeric Biomaterials, Revised and Expanded*. (CRC Press, 2001).
7. Akiba, M. & Hashim, A. S. Vulcanization and crosslinking in elastomers. *Prog. Polym. Sci.* **22**, 475-521 (1997).
8. Giusto, J. D. *Vascular Access Catheter Materials and Evolution*. (Xlibris US, 2014).
9. de Buyl, F. Silicone sealants and structural adhesives. *Int. J. Adhes. Adhes.* **21**, 411-422 (2001).
10. Ratner, B. D. *et al. Biomedical Engineering e-Mega Reference*. (Elsevier Science, 2009).
11. El-Zaim, H. & Heggors, J. in *Polymeric Biomaterials, Revised and Expanded* (CRC Press, 2001). doi:doi:10.1201/9780203904671.ch3
12. Ansarifar, A., Azhar, A., Ibrahim, N., Shiah, S. F. & Lawton, J. M. D. The use of a silanised silica filler to reinforce and crosslink natural rubber. *Int. J. Adhes. Adhes.* **25**, 77-86 (2005).
13. Bhowmick, A. K. & Stephens, H. *Handbook of Elastomers, Second Edition*,. (Taylor & Francis, 2000).
14. Saleem, H. *et al.* Mechanical and Thermal Properties of Thermoset-Graphene Nanocomposites. *Macromol. Mater. Eng.* **301**, 231-259 (2016).
15. Lobo, S., Sachdeva, S. & Goswami, T. Role of pressure-sensitive adhesives in transdermal drug delivery systems. *Ther. Deliv.* **7**, 33-48 (2016).
16. Stapleton, F., Stretton, S., Papas, E., Skotnitsky, C. & Sweeney, D. F. Silicone hydrogel contact lenses and the ocular surface. *Ocul. Surf.* **4**, 24-43 (2006).
17. Raghu, K. M., Gururaju, C. R., Sundaresh, K. J. & Mallikarjuna, R. Aesthetic finger prosthesis with silicone biomaterial. *BMJ Case Reports* **2013**, (2013).
18. Chao, A. H., Garza R., I. I. I. & Povoski, S. P. A review of the use of silicone implants in breast surgery. *Expert Rev. Med. Devices* **13**, 143-156 (2016).
19. Bodiwala, D., Summerton, D. J. & Terry, T. R. Testicular prostheses: Development and modern usage. *Ann. R. Coll. Surg. Engl.* **89**, 349-353 (2007).
20. Soares, D. J. & Silver, W. E. Midface skeletal enhancement. *Facial Plast. Surg. Clin. North Am.* **23**, 185-193 (2015).
21. Criner, K. T. & Ilyas, A. M. Silicone arthroplasty for chronic proximal interphalangeal joint dislocations. *Tech. Hand Up. Extrem. Surg.* **15**, 209-214 (2011).
22. Namdari, S. & Weiss, A.-P. C. Anatomically Neutral Silicone Small Joint Arthroplasty for Osteoarthritis. *J. Hand Surg. Am.* **34**, 292-300 (2009).

23. Iida, M. *et al.* A newly developed silicone-coated membrane oxygenator for long-term cardiopulmonary bypass and cardiac support. *Artif. Organs* **21**, 755-759 (1997).
24. Zhong, S. P., Zhang, Y. Z. & Lim, C. T. Tissue scaffolds for skin wound healing and dermal reconstruction. *Wiley Interdiscip. Rev. Nanomedicine Nanobiotechnology* **2**, 510-525 (2010).
25. Abbasi, F., Mirzadeh, H. & Katbab, A.-A. Modification of polysiloxane polymers for biomedical applications: a review. *Polym. Int.* **50**, 1279-1287 (2001).
26. Gad, S. C. & Gad-McDonald, S. *Biomaterials, Medical Devices, and Combination Products: Biocompatibility Testing and Safety Assessment*. (CRC Press, 2015).
27. Salama, F. A. Application of polymers in urology. in *International SAMPE Symposium and Exhibition (Proceedings)* **38**, 573-581 (1993).
28. Oliver, M. J. Acute dialysis catheters. *Semin. Dial.* **14**, 432-435 (2001).
29. Gray, R. J. & Sands, J. J. *Dialysis Access: A Multidisciplinary Approach*. (Lippincott Williams & Wilkins, 2002).
30. Ronco, C. & Levin, N. W. *Hemodialysis, Vascular Access, and Peritoneal Dialysis Access*. (Karger, 2004).
31. Bhat, S. V. *Biomaterials*. (Springer Netherlands, 2012).
32. Wacker Chemie AG. *Solid and Liquid Silicone Rubber: Material and Processing Guidelines*. (2016).
33. Dow Corning. *Moulding of SILASTIC Silicone Rubber*. (2016).
34. Bhowmick, A. K. *Current Topics in Elastomers Research*. (CRC Press, 2008).
35. Owen, M. J. & Smith, P. J. Plasma treatment of polydimethylsiloxane. *J. Adhes. Sci. Technol.* **8**, 1063-1075 (1994).
36. Williams, R. L., Wilson, D. J. & Rhodes, N. P. Stability of plasma-treated silicone rubber and its influence on the interfacial aspects of blood compatibility. *Biomaterials* **25**, 4659-4673 (2004).
37. Owen, M. J. & Dvornic, P. R. *Silicone Surface Science*. (Springer Netherlands, 2012).
38. Ouyang, M., Yuan, C., Muisener, R. J., Boulares, A. & Koberstein, J. T. Conversion of Some Siloxane Polymers to Silicon Oxide by UV/Ozone Photochemical Processes. *Chem. Mater.* **12**, 1591-1596 (2000).
39. Syring, A., Fricke-Begemann, T. & Ihlemann, J. F2-laser modification and patterning of silicone films. *Appl. Surf. Sci.* **261**, 68-74 (2012).
40. Goddard, J. M. & Hotchkiss, J. H. Polymer surface modification for the attachment of bioactive compounds. *Prog. Polym. Sci.* **32**, 698-725 (2007).
41. Bambauer, R., Latza, R., Bambauer, S. & Tobin, E. Large Bore Catheters with Surface Treatments versus Untreated Catheters for Vascular Access in Hemodialysis. *Artif. Organs* **28**, 604-610 (2004).
42. Yoshiaki, S., Masahiro, K. & Masaya, I. Surface analysis of antithrombogenic ion-implanted silicone rubber. *Nucl. Instruments Methods Phys. Res. Sect. B Beam Interact. with Mater. Atoms* **59**, 1300-1303 (1991).
43. Atala, A. *Foundations of Regenerative Medicine: Clinical and Therapeutic Applications*. (Elsevier Science, 2009).
44. Liu, X., Xu, Y., Wu, Z. & Chen, H. Poly(N-vinylpyrrolidone)-Modified surfaces for biomedical applications. *Macromol. Biosci.* **13**, 147-154 (2013).
45. Magaña, H. *et al.* Radiation-grafting of acrylamide onto silicone rubber films for diclofenac delivery. *Radiat. Phys. Chem.* **107**, 164-170 (2015).
46. Meléndez-Ortiz, H. I. *et al.* Radiation-grafting of N-vinylimidazole onto silicone rubber for antimicrobial properties. *Radiat. Phys. Chem.* **110**, 59-66 (2015).
47. Bennett, D. R., Stark, F. O. & Vogel, G. E. Anticoagulant surfaces produced by radiation grafting heparin to a silicone substrate. (1969).
48. D'Sa, R. A. *et al.* Atmospheric pressure plasma induced grafting of poly(ethylene glycol) onto silicone elastomers for controlling biological response. *J. Colloid Interface Sci.* **375**, 193-202 (2012).
49. Li, X. *et al.* Antimicrobial functionalization of silicone surfaces with engineered

- short peptides having broad spectrum antimicrobial and salt-resistant properties. *Acta Biomater.* **10**, 258-266 (2014).
50. Xu, J., Yuan, Y., Shan, B., Shen, J. & Lin, S. Ozone-induced grafting phosphorylcholine polymer onto silicone film grafting 2-methacryloyloxyethyl phosphorylcholine onto silicone film to improve hemocompatibility. *Colloids Surfaces B Biointerfaces* **30**, 215-223 (2003).
 51. Fakirov, S. *Nano-size Polymers: Preparation, Properties, Applications*. (Springer International Publishing, 2016).
 52. Bloomfield, L. A. Primer system for bonding conventional adhesives and coatings to silicone rubber. *Int. J. Adhes. Adhes.* **68**, 239-247 (2016).
 53. Fortuniak, W. *et al.* Polysiloxanes With Quaternary Ammonium Salt Biocidal Functions and Their Behavior When Incorporated Into a Silicone Elastomer Network. *J. Inorg. Organomet. Polym. Mater.* **21**, 576 (2011).
 54. Ye, S., Majumdar, P., Chisholm, B., Stafslie, S. & Chen, Z. Antifouling and Antimicrobial Mechanism of Tethered Quaternary Ammonium Salts in a Cross-linked Poly(dimethylsiloxane) Matrix Studied Using Sum Frequency Generation Vibrational Spectroscopy. *Langmuir* **26**, 16455-16462 (2010).
 55. Stickler, D. J. in *Coatings for Biomedical Applications* (ed. Driver, M.) 304-335 (Woodhead Publishing, 2012). doi:http://dx.doi.org/10.1533/9780857093677.2.304
 56. Wang, R., Neoh, K. G., Kang, E.-T., Tambyah, P. A. & Chiong, E. Antifouling coating with controllable and sustained silver release for long-term inhibition of infection and encrustation in urinary catheters. *J. Biomed. Mater. Res. Part B Appl. Biomater.* **103**, 519-528 (2015).
 57. Geim, A. K. Graphene: Status and Prospects. *Science (80-.)*. **324**, 1530-1534 (2009).
 58. Sadasivuni, K. K., Ponnamm, D., Thomas, S. & Grohens, Y. Evolution from graphite to graphene elastomer composites. *Prog. Polym. Sci.* **39**, 749-780 (2014).
 59. Papageorgiou, D. G., Kinloch, I. A. & Young, R. J. Graphene/elastomer nanocomposites. *Carbon N. Y.* **95**, 460-484 (2015).
 60. Tong, Y., Bohmb, S. & Song, M. Graphene Based Materials and Their Composites as Coatings. *Austin J. Nanomedicine Nanotechnol.* **1**, 1-16 (2013).
 61. Shen, H., Zhang, L., Liu, M. & Zhang, Z. Biomedical Applications of Graphene. *Theranostics* **2**, 283-294 (2012).
 62. Singh, V. *et al.* Graphene based materials: Past, present and future. *Prog. Mater. Sci.* **56**, 1178-1271 (2011).
 63. Lukowiak, A., Kedziora, A. & Streck, W. Antimicrobial graphene family materials: Progress, advances, hopes and fears. *Adv. Colloid Interface Sci.* **236**, 101-112 (2016).
 64. Pumera, M. Electrochemistry of graphene: new horizons for sensing and energy storage. *Chem. Rec.* **9**, 211-223 (2009).
 65. Wan, Q. *et al.* Graphene nanoplatelets: Electrochemical properties and applications for oxidation of endocrine-disrupting chemicals. *Chem. - A Eur. J.* **19**, 3483-3489 (2013).
 66. Kuilla, T. *et al.* Recent advances in graphene based polymer composites. *Prog. Polym. Sci.* **35**, 1350-1375 (2010).
 67. Kim, J. *et al.* Graphene-based waveguides: Novel method for detecting biological activity. *Appl. Biochem. Biotechnol.* **167**, 1069-1075 (2012).
 68. Lin, Z., Hu, X. & Ke, Y. Transparent graphene/phenyl-silicone rubber composites for LED packaging materials. *Fuhe Cailiao Xuebao/Acta Mater. Compos. Sin.* **33**, 2054-2060 (2016).
 69. Hou, S. *et al.* Formation of highly stable dispersions of silane-functionalized reduced graphene oxide. *Chem. Phys. Lett.* **501**, 68-74 (2010).
 70. Lordeus, M. *et al.* Graphene nanoplatelet-reinforced silicone for the valvular prosthesis application. *J. Long. Term. Eff. Med. Implants* **25**, 95-103 (2015).
 71. Lin, F. *et al.* Substrate effect modulates adhesion and proliferation of fibroblast on

- graphene layer. *Colloids Surfaces B Biointerfaces* **146**, 785-793 (2016).
72. Koo, C. M. Graphene Electrodes for Artificial Muscles. (2014). doi:10.1080/15421406.2011.566507
 73. Zhang, G., Wang, F., Dai, J. & Huang, Z. Effect of Functionalization of Graphene Nanoplatelets on the Mechanical and Thermal Properties of Silicone Rubber Composites. *Materials (Basel)*. **9**, 92 (2016).
 74. Gan, L., Shang, S., Yuen, C. W. M., Jiang, S. & Luo, N. M. Facile preparation of graphene nanoribbon filled silicone rubber nanocomposite with improved thermal and mechanical properties. *Compos. Part B Eng.* **69**, 237-242 (2015).
 75. Valentini, L., Bon, S. B. & Pugno, N. M. Severe graphene nanoplatelets aggregation as building block for the preparation of negative temperature coefficient and healable silicone rubber composites. *Compos. Sci. Technol.* **134**, 125-131 (2016).
 76. Song, Y. *et al.* Enhancing the thermal, electrical, and mechanical properties of silicone rubber by addition of graphene nanoplatelets. *Mater. Des.* **88**, 950-957 (2015).
 77. Zhao, X., Zang, C., Wen, Y. & Jiao, Q. Thermal and mechanical properties of liquid silicone rubber composites filled with functionalized graphene oxide. *J. Appl. Polym. Sci.* **132**, (2015).
 78. Dong, J., Wang, P. H., Sun, D. B., Xu, Y. L. & Li, K. P. Preparation and Characterization of Graphene/RTV Silicone Rubber Composites. *Adv. Mater. Res.* **652-654**, 11-14 (2013).
 79. Li, W., Gedde, U. W. & Hillborg, H. Structure and electrical properties of silicone rubber filled with thermally reduced graphene oxide. *IEEE Transactions on Dielectrics and Electrical Insulation* **23**, 1156-1163 (2016).
 80. Bai, Y., Cai, H., Qiu, X., Fang, X. & Zheng, J. Effects of graphene reduction degree on thermal oxidative stability of reduced graphene oxide/silicone rubber nanocomposites. *High Perform. Polym.* **27**, 997-1006 (2015).
 81. Zong, Y. *et al.* Preparation and thermo-mechanical properties of functionalized graphene/silicone rubber nanocomposites. *2015 16th International Conference on Electronic Packaging Technology (ICEPT)* 30-34 (2015). doi:10.1109/ICEPT.2015.7236538
 82. Ma, W., Li, J., Deng, B., Lin, X. & Zhao, X. Properties of functionalized graphene/room temperature vulcanized silicone rubber composites prepared by an In-situ reduction method. *J. Wuhan Univ. Technol. Sci. Ed.* **28**, 127-131 (2013).
 83. Ozbas, B. *et al.* Multifunctional elastomer nanocomposites with functionalized graphene single sheets. *J. Polym. Sci. Part B Polym. Phys.* **50**, 910-916 (2012).
 84. He, Q. *et al.* Adhesion characteristics of a novel synthetic polydimethylsiloxane for bionic adhesive pads. *J. Bionic Eng.* **11**, 371-377 (2014).
 85. Zou, X., Zhang, L., Wang, Z. & Luo, Y. Mechanisms of the Antimicrobial Activities of Graphene Materials. *J. Am. Chem. Soc.* **138**, 2064-2077 (2016).
 86. Hegab, H. M. *et al.* The controversial antibacterial activity of graphene-based materials. *Carbon N. Y.* **105**, 362-376 (2016).
 87. Szunerits, S. & Boukherroub, R. Antibacterial activity of graphene-based materials. *J. Mater. Chem. B* **4**, 6892-6912 (2016).
 88. Li, J. *et al.* Antibacterial activity of large-area monolayer graphene film manipulated by charge transfer. *Sci. Rep.* **4**, 4359 (2014).
 89. Ji, H., Sun, H. & Qu, X. Antibacterial applications of graphene-based nanomaterials: Recent achievements and challenges. *Adv. Drug Deliv. Rev.* **105**, 176-189 (2016).
 90. Rojas-Andrade, M. D. *et al.* Antibacterial mechanisms of graphene-based composite nanomaterials. *Nanoscale* 994-1006 (2017). doi:10.1039/C6NR08733G
 91. Yousefi, M. *et al.* Anti-bacterial activity of graphene oxide as a new weapon nanomaterial to combat multidrug-resistance bacteria. *Mater. Sci. Eng. C* **74**, 568-581 (2017).
 92. Parra, C. *et al.* Suppressing Bacterial Interaction with Copper Surfaces through

- Graphene and Hexagonal-Boron Nitride Coatings. *ACS Appl. Mater. Interfaces* **7**, 6430-6437 (2015).
93. Saud, S. N. *et al.* Corrosion and bioactivity performance of graphene oxide coating on TiNb shape memory alloys in simulated body fluid. *Mater. Sci. Eng. C* **68**, 687-694 (2016).
 94. Perreault, F., de Faria, A. F., Nejati, S. & Elimelech, M. Antimicrobial Properties of Graphene Oxide Nanosheets: Why Size Matters. *ACS Nano* **9**, 7226-7236 (2015).
 95. Santos, C. M. *et al.* Graphene nanocomposite for biomedical applications: fabrication, antimicrobial and cytotoxic investigations. *Nanotechnology* **23**, 395101 (2012).
 96. Santos, C. M. *et al.* Antimicrobial graphene polymer (PVK-GO) nanocomposite films. *Chem. Commun. (Camb)*. **47**, 8892-8894 (2011).
 97. Krishnamoorthy, K. *et al.* Graphene oxide nanopaint. *Carbon N. Y.* **72**, 328-337 (2014).
 98. Zhao, C. *et al.* Graphene oxide based coatings on nitinol for biomedical implant applications: effectively promote mammalian cell growth but kill bacteria. *RSC Adv.* **6**, 38124-38134 (2016).
 99. Karimi, L., Yazdanshenas, M. E., Khajavi, R., Rashidi, A. & Mirjalili, M. Using graphene/TiO₂ nanocomposite as a new route for preparation of electroconductive, self-cleaning, antibacterial and antifungal cotton fabric without toxicity. *Cellulose* **21**, 3813-3827 (2014).
 100. Sun, X.-F. *et al.* Graphene oxide-silver nanoparticle membrane for biofouling control and water purification. *Chem. Eng. J.* **281**, 53-59 (2015).
 101. Janković, A. *et al.* Graphene-based antibacterial composite coatings electrodeposited on titanium for biomedical applications. *Prog. Org. Coatings* **83**, 1-10 (2015).
 102. Correa, C. F. *et al.* Antimicrobial activity from polymeric composites-based polydimethylsiloxane/TiO₂/GO: evaluation of filler synthesis and surface morphology. *Polym. Bull.* 1-12 (2016). doi:10.1007/s00289-016-1843-8
 103. Magennis, E. P. *et al.* Engineering serendipity: High-throughput discovery of materials that resist bacterial attachment(). *Acta Biomater.* **34**, 84-92 (2016).
 104. Napalkov, P., Felici, D. M., Chu, L. K., Jacobs, J. R. & Begelman, S. M. Incidence of catheter-related complications in patients with central venous or hemodialysis catheters: a health care claims database analysis. *BMC Cardiovasc. Disord.* **13**, 86 (2013).
 105. Zhang, H. & Chiao, M. Anti-fouling Coatings of Poly(dimethylsiloxane) Devices for Biological and Biomedical Applications. *Journal of Medical and Biological Engineering* **35**, 143-155 (2015).
 106. Salwiczek, M. *et al.* Emerging rules for effective antimicrobial coatings. *Trends Biotechnol.* **32**, 82-90 (2014).
 107. O'Toole, G., Kaplan, H. B. & Kolter, R. Biofilm Formation as Microbial Development. *Annu. Rev. Microbiol.* **54**, 49-79 (2000).
 108. Shaw, P., Shaw, C. K. & Saileela, K. Correlation between intravenous catheter related infections and biofilms in *Staphylococcus epidermidis*. *Int. J. Pharma Bio Sci.* **3**, B638-B646 (2012).
 109. Campoccia, D., Montanaro, L. & Arciola, C. R. A review of the biomaterials technologies for infection-resistant surfaces. *Biomaterials* **34**, 8533-8554 (2013).
 110. Yu, Q., Wu, Z. & Chen, H. Dual-function antibacterial surfaces for biomedical applications. *Acta Biomater.* **16**, 1-13 (2015).
 111. Hasan, J., Crawford, R. J. & Ivanova, E. P. Antibacterial surfaces: the quest for a new generation of biomaterials. *Trends Biotechnol.* **31**, 295-304 (2013).
 112. ISO. ISO 22196: Plastics – Measurement of antibacterial activity on plastics surfaces. (2007).
 113. ASTM. ASTM E2180-07: Standard Test Method for Determining the Activity of

- Incorporated Antimicrobial Agent(s) In Polymeric or Hydrophobic Materials,. (2012).
114. Hazan, R., Que, Y.-A., Maura, D. & Rahme, L. G. A method for high throughput determination of viable bacteria cell counts in 96-well plates. *BMC Microbiol.* **12**, 259 (2012).
 115. Trampuz, A., Salzman, S., Antheaume, J. & Daniels, A. U. Microcalorimetry: a novel method for detection of microbial contamination in platelet products. *Transfusion* **47**, 1643-1650 (2007).
 116. Rio, L. *et al.* Comparison of methods for evaluation of the bactericidal activity of copper-sputtered surfaces against methicillin-resistant *Staphylococcus aureus*. *Appl. Environ. Microbiol.* **78**, 8176-82 (2012).
 117. Braissant, O. *et al.* Isothermal microcalorimetry accurately detects bacteria, tumorous microtissues, and parasitic worms in a label-free well-plate assay. *Biotechnol. J.* **10**, 460-468 (2015).
 118. Berridge, M. V & Tan, A. S. Characterization of the cellular reduction of 3-(4,5-dimethylthiazol-2-yl)-2,5-diphenyltetrazolium bromide (MTT): subcellular localization, substrate dependence, and involvement of mitochondrial electron transport in MTT reduction. *Arch. Biochem. Biophys.* **303**, 474-482 (1993).
 119. Wang, H., Cheng, H., Wang, F., Wei, D. & Wang, X. An improved 3-(4,5-dimethylthiazol-2-yl)-2,5-diphenyl tetrazolium bromide (MTT) reduction assay for evaluating the viability of *Escherichia coli* cells. *J. Microbiol. Methods* **82**, 330-333 (2010).
 120. Gobor, T. *et al.* Proposal of protocols using D-glutamine to optimize the 2,3-bis(2-methoxy-4-nitro-5-sulfophenyl)-5-[(phenylamino) carbonyl]-2H-tetrazolium hydroxide (XTT) assay for indirect estimation of microbial loads in biofilms of medical importance. *J. Microbiol. Methods* **84**, 299-306 (2011).
 121. Abelson, J. N., Simon, M. I. & Doyle, R. J. *Biofilms*. (Elsevier Science, 1999).
 122. Sarker, S. D., Nahar, L. & Kumarasamy, Y. Microtitre plate-based antibacterial assay incorporating resazurin as an indicator of cell growth, and its application in the in vitro antibacterial screening of phytochemicals. *Methods (San Diego, Calif.)* **42**, 321-324 (2007).
 123. Hudman, D. A. & Sargentini, N. J. Resazurin-based assay for screening bacteria for radiation sensitivity. *SpringerPlus* **2**, (2013).
 124. Mariscal, A., Lopez-Gigosos, R. M., Carnero-Varo, M. & Fernandez-Crehuet, J. Fluorescent assay based on resazurin for detection of activity of disinfectants against bacterial biofilm. *Appl. Microbiol. Biotechnol.* **82**, 773-783 (2009).
 125. Leroy, C. *et al.* A marine bacterial adhesion microplate test using the DAPI fluorescent dye: a new method to screen antifouling agents. *Lett. Appl. Microbiol.* **44**, 372-378 (2007).
 126. Long, N., Wong, W. T. & Immergut, E. H. *The Chemistry of Molecular Imaging*. (Wiley, 2014).
 127. Paul, J. H. Use of hoechst dyes 33258 and 33342 for enumeration of attached and planktonic bacteria. *Appl. Environ. Microbiol.* **43**, 939-944 (1982).
 128. Tarnowski, B. I., Spinale, F. G. & Nicholson, J. H. DAPI as a useful stain for nuclear quantitation. *Biotech. Histochem.* **66**, 296-302 (1991).
 129. Stocks, S. M. Mechanism and use of the commercially available viability stain, BacLight. *Cytom. Part A* **61A**, 189-195 (2004).
 130. Almeida, C., Azevedo, N. F., Santos, S., Keevil, C. W. & Vieira, M. J. Discriminating Multi-Species Populations in Biofilms with Peptide Nucleic Acid Fluorescence In Situ Hybridization (PNA FISH). *PLoS One* **6**, 1-13 (2011).
 131. Cushnie, T. P. T., O'Driscoll, N. H. & Lamb, A. J. Morphological and ultrastructural changes in bacterial cells as an indicator of antibacterial mechanism of action. *Cell. Mol. Life Sci.* **73**, 4471-4492 (2016).
 132. Koseki, H. *et al.* Early *Staphylococcal* Biofilm Formation on Solid Orthopaedic Implant Materials: In Vitro Study. *PLoS One* **9**, e107588 (2014).

133. Zaura, E. & Mira, A. *The Oral Microbiome in an Ecological Perspective*: (Frontiers Media SA, 2015).
134. Hummers, W. S. & Offeman, R. E. Preparation of Graphitic Oxide. *J. Am. Chem. Soc.* **80**, 1339 (1958).
135. Marcano, D. C. *et al.* Improved Synthesis of Graphene Oxide. *ACS Nano* **4**, 4806-4814 (2010).
136. Shen, X., Lin, X., Yousefi, N., Jia, J. & Kim, J.-K. Wrinkling in graphene sheets and graphene oxide papers. *Carbon N. Y.* **66**, 84-92 (2014).
137. Geng, Y., Wang, S. J. & Kim, J. Journal of Colloid and Interface Science Preparation of graphite nanoplatelets and graphene sheets. *J. Colloid Interface Sci.* **336**, 592-598 (2009).
138. Stobinski, L., Lesiak, B., Malolepszy, A., Mazurkiewicz, M. & Mierzwa, B. Journal of Electron Spectroscopy and Graphene oxide and reduced graphene oxide studied by the XRD , TEM and electron spectroscopy methods. *J. Electron Spectros. Relat. Phenomena* **195**, 145-154 (2014).
139. Pinto, A. M., Gonçalves, C., Sousa, D. M., Ferreira, A. R. & Magalh, D. Smaller particle size and higher oxidation improves biocompatibility of graphene-based materials. **99**, 318-329 (2016).
140. Thermo Scientific XPS. Carbon. Available at: <http://xpssimplified.com/elements/carbon.php#appnotes>. (Accessed: 25th June 2017)
141. Chuah, Y. J. *et al.* Simple surface engineering of polydimethylsiloxane with polydopamine for stabilized mesenchymal stem cell adhesion and multipotency. *Nat. Publ. Gr.* 1-12 (2015). doi:10.1038/srep18162
142. Bayles, K. W. The biological role of death and lysis in biofilm development. *Nat. Rev. Microbiol.* **5**, 721-726 (2007).
143. Zheng, Q. & Lü, C. Size Effects of Surface Roughness to Superhydrophobicity. *Procedia IUTAM* **10**, 462-475 (2014).
144. Kim, T. I. *et al.* Antibacterial Activities of Graphene Oxide-Molybdenum Disulfide Nanocomposite Films. *ACS Appl. Mater. Interfaces* **9**, 7908-7917 (2017).

Annexes

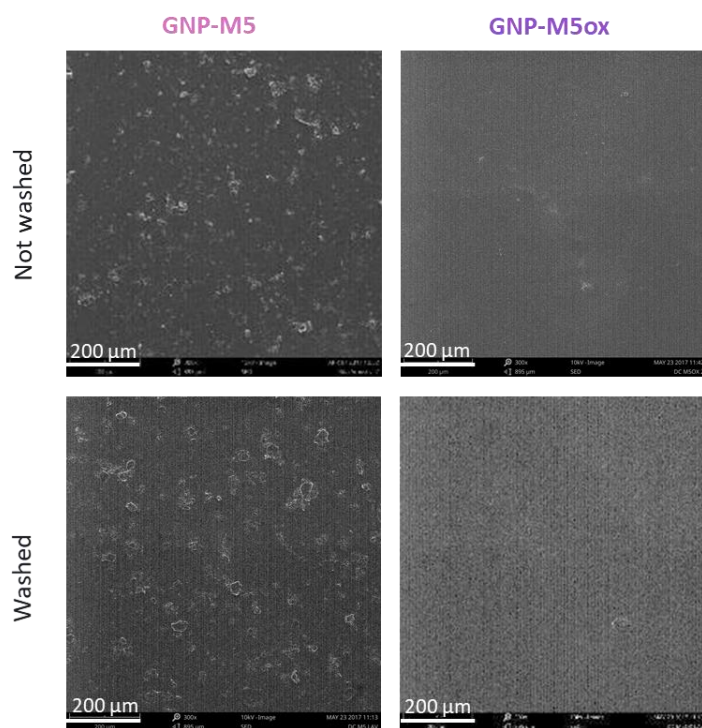


Figure A1. SEM images of SR/GNP dip coating surfaces of 2 mg/mL concentrations before and after the washing test. Pictures taken at the magnification of $\times 300$. (Scale bar = 200 μm).

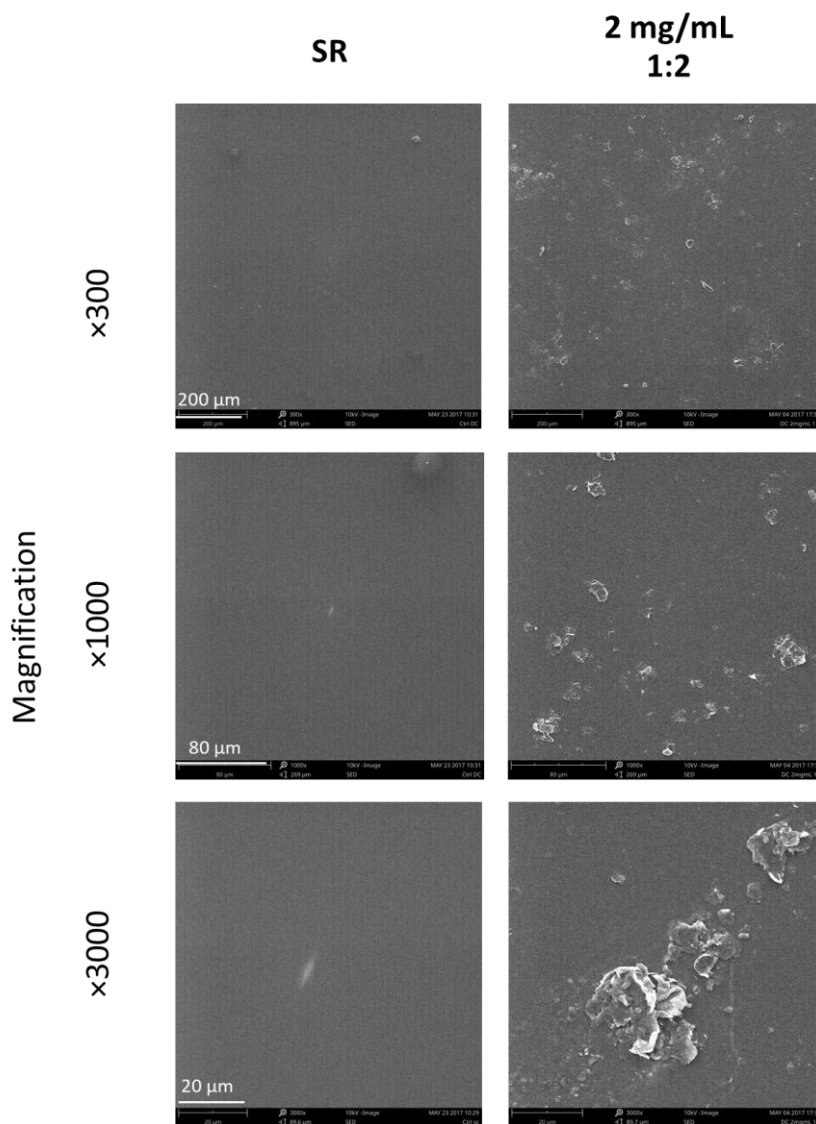


Figure A2. SEM images of SR/GNP-M5 dip coating samples in the proportion of 1:2. Pictures taken at the magnifications of $\times 300$, $\times 1000$ and $\times 3000$ (Scale bar= 200 μm , 80 μm and 20 μm , respectively).

Table A1. Total adhered bacteria/mm² statistical analysis for TCPET in dip coating antimicrobial assay. Statistical analysis performed with ordinary one-way ANOVA test and differences are indicated with * ($p \leq 0.05$), ** ($p \leq 0.01$), *** ($p \leq 0.001$) and **** ($p \leq 0.0001$).

Tukey's multiple comparisons test	Mean Diff.	95% CI of diff.	Significant?	Summary
TCPET vs. SRf	-20.55	-229.0 to 187.9	No	ns
TCPET vs. SR	-5.715	-202.8 to 191.3	No	ns
TCPET vs. SR/GNP-M5 1 mg/mL	69.95	-157.0 to 296.9	No	ns
TCPET vs. SR/GNP-M5 2 mg/mL	-431.8	-640.3 to -223.4	Yes	****
TCPET vs. SR/GNP-M5ox 1 mg/mL	-16.18	-246.4 to 214.1	No	ns
TCPET vs. SR/GNP-M5ox 2 mg/mL	-301.1	-502.5 to -99.65	Yes	***

Table A2. CFU counts for the initial inoculum and recovery rate for SR dip coating samples.

Initial inoculum	
	5.50E+05
	3.60E+05
AVERAGE	4.67E+05
SD	9.71E+04

Recovery rate	
1º REPLICA (CFUs/mL)	3.33E+05
	3.93E+05
	3.47E+05
2º REPLICA (CFUs/mL)	4.07E+05
	4.87E+05
	3.40E+05
3º REPLICA (CFUs/mL)	3.80E+05
	4.47E+05
	4.53E+05
AVERAGE	3.99E+05
SD	5.46E+04

Table A3. CFU counts statistical analysis for TCPET in dip coating antimicrobial assay. Statistical analysis performed with ordinary one-way ANOVA and differences are indicated with * ($p \leq 0.05$), ** ($p \leq 0.01$), *** ($p \leq 0.001$) and **** ($p \leq 0.0001$).

Tukey's multiple comparisons test	Mean Diff.	95% CI of diff.	Significant?	Summary
TCPET vs. SRf	-1.31E+09	-2.170e+009 to -4.470e+008	Yes	***
TCPET vs. SR	-1.48E+09	-2.343e+009 to -6.203e+008	Yes	****
TCPET vs. SR/GNP-M5 1 mg/mL	-4.30E+07	-9.044e+008 to 8.184e+008	No	ns
TCPET vs. SR/GNP-M5 2 mg/mL	-3.80E+08	-1.242e+009 to 4.810e+008	No	ns
TCPET vs. SR/GNP-M5ox 1 mg/mL	-2.01E+09	-2.870e+009 to -1.148e+009	Yes	****
TCPET vs. SR/GNP-M5ox 2 mg/mL	-1.87E+09	-2.727e+009 to -1.004e+009	Yes	****

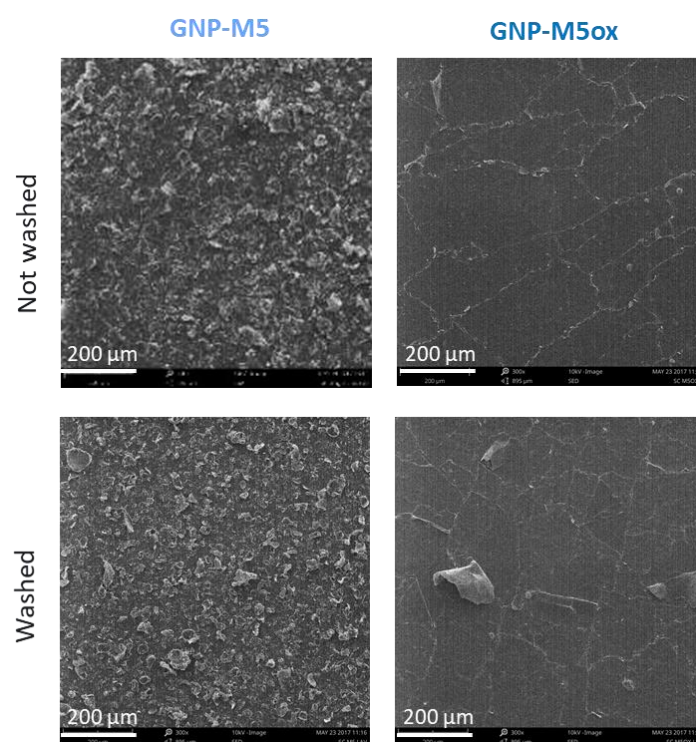


Figure A2. SEM images of SR/GNP spray coating surfaces of 2 mg/mL concentrations before and after the washing test. Pictures taken at the magnification of $\times 300$. (Scale bar = 200 μm).

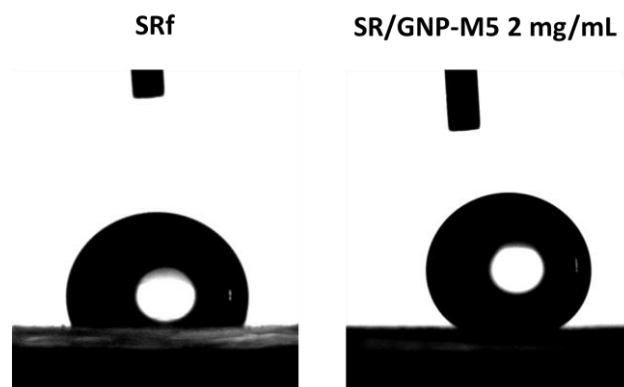


Figure A3. Contact angle images of SRf and SR/GNP-M5 2 mg/mL.

Table A4. Total adhered bacteria/mm² statistical analysis for TCPET in spray coating antimicrobial assay. Statistical analysis performed with ordinary one-way ANOVA test and differences are indicated with * ($p \leq 0.05$), ** ($p \leq 0.01$), *** ($p \leq 0.001$) and **** ($p \leq 0.0001$).

Tukey's multiple comparisons test	Mean Diff.	95% CI of diff.	Significant?	Summary
TCPET vs. SRf	-2.45	-208.1 to 203.2	No	ns
TCPET vs. SR	-129.6	-335.6 to 76.46	No	ns
TCPET vs. SR/GNP-M5 0.5 mg/mL	-415.7	-621.4 to -210.0	Yes	****
TCPET vs. SR/GNP-M5 1mg/mL	-1363	-1601 to -1125	Yes	****
TCPET vs. SR/GNP-M5ox 0.5 mg/mL	-302.5	-521.3 to -83.71	Yes	***
TCPET vs. SR/GNP-M5ox 1 mg/mL	-950.4	-1156 to -744.4	Yes	****

Table A5. CFU counts for the initial inoculum and recovery rate for SR spray coating samples.

Initial inoculum	
	5.10E+05
	5.70E+05
AVERAGE	5.63E+05
SD	5.03E+04

Recovery rate	
1º REPLICA (CFUs/mL)	5.73E+05
	4.60E+05
	5.13E+05
2º REPLICA (CFUs/mL)	5.33E+05
	4.87E+05
	4.73E+05
3º REPLICA (CFUs/mL)	4.40E+05
	4.73E+05
	4.13E+05
AVERAGE	4.85E+05
SD	4.87E+04

Table A 6. CFU counts statistical analysis for TCPET in spray coating antimicrobial assay. Statistical analysis performed with ordinary one-way ANOVA and differences are indicated with * ($p \leq 0.05$), ** ($p \leq 0.01$), * ($p \leq 0.001$) and **** ($p \leq 0.0001$).**

Tukey's multiple comparisons test	Mean Diff.	95% CI of diff.	Significant?	Summary
TCPET vs. SRf	1.35E+09	5.209e+008 to 2.169e+009	Yes	****
TCPET vs. SR	1.19E+09	2.964e+008 to 2.083e+009	Yes	**
TCPET vs. SR/GNP-M5 0.5 mg/mL	1.99E+09	1.164e+009 to 2.812e+009	Yes	****
TCPET vs. SR/GNP-M5 1 mg/mL	1.13E+09	3.069e+008 to 1.955e+009	Yes	**
TCPET vs. SR/GNP-M5ox 0.5 mg/mL	6.08E+07	-7.631e+008 to 8.846e+008	No	ns
TCPET vs. SR/GNP-M5ox 1 mg/mL	-9.01E+08	-1.724e+009 to -7.673e+007	Yes	*